Pooled clone collections by multiplexed CRISPR/Cas12a-assisted gene tagging in yeast

Benjamin C. Buchmuller[1,4], Konrad Herbst[1,4], Matthias Meurer[1], Daniel Kirrmaier[1,3], Ehud Sass[2], Emmanuel D. Levy[2], Michael Knop[1,3]

[1] Zentrum für Molekulare Biologie der Universität Heidelberg (ZMBH), DKFZ-ZMBH Alliance, Heidelberg, Germany.

[2] Department of Structural Biology, Weizmann Institute of Science, Rehovot, Israel.

[3] Cell Morphogenesis and Signal Transduction, German Cancer Research Center (DKFZ), DKFZ-ZMBH Alliance, Heidelberg, Germany.

[4] These authors contributed equally.

Correspondence should be addressed to M.K. (m.knop@zmbh.uni-heidelberg.de).

Abstract

Clone collections of modified strains ('libraries') are a major resource for systematic studies with the yeast *Saccharomyces cerevisiae*. Construction of such libraries is time-consuming, costly and confined to the genetic background of a specific yeast strain. To overcome these limitations, we developed CRISPR/Cas12a (Cpf1)-assisted tag library engineering (CASTLING) for multiplexed strain construction. CASTLING uses microarray-synthesized oligonucleotide pools and *in vitro* recombineering to program the genomic insertion of long DNA constructs via homologous recombination. One simple transformation yields pooled libraries with >90% of correctly tagged clones. Up to several hundred genes can be tagged in a single step and, on a genomic scale, approximately half of all genes are tagged with only ~10-fold oversampling. We report several parameters that affect tagging success and provide a quantitative targeted next-generation sequencing method to analyze such pooled collections. Thus, CASTLING unlocks new avenues for increased throughput in functional genomics and cell biology research. (max 150 words)

Introduction

The systematic screening of arrayed biological resources in high-throughput has proven highly informative and valuable to disentangle gene and protein function. For eukaryotic cells, a large body of such data has been obtained from yeast strain collections ('libraries') in which thousands of open reading frames (ORFs) are systematically altered in identical ways, e.g. by gene inactivation or over-expression to determine gene dosage phenotypes and genetic interactions[1-3]. Likewise, gene tagging, e.g. with fluorescent protein reporters, has been used in functional genomics to study protein abundance[4], localization[5], turnover[6,7], or protein-protein interactions[8-10].

Due to their gene-wise construction, producing arrayed clone collections is typically time-consuming and cost-intensive. For yeast, this has been partly addressed with the development of 'SWAT libraries' in which a generic 'SWAp Tag' can be systematically replaced with the desired reporter for N- or C-terminal tagging any ORF in the genome[11,12]. However, manipulation and screening of arrayed libraries remains dependent on special equipment to handle the strain collections and is ultimately confined to the genetic background of the yeast strain BY4741[13] in which most of these libraries were constructed. Therefore, arrayed libraries do not address current and future demands in functional genomics that embrace the systematic analysis of complex traits or the comparison of different strains or species[14]. We imagine that a paradigm shift from arrayed to pooled library generation may offer a solution since experimentation with pooled biological resources is already well established, e.g., in chemical genomics[15].

To bridge this gap, efficient means are required for generating pooled libraries rapidly and independently of the genetic background. For example, RNA-programmable CRISPR endonucleases have revolutionized the creation of pooled collections of gene activation and inactivation mutants in mammalian cells[16-18]. By using thousands of CRISPR guide RNAs (gRNAs) easily produced by cost-effective microarray-based oligonucleotide synthesis these libraries can be quickly constructed. The pooled library is then enriched for the desired phenotypes and quantitatively assessed by next-generation sequencing (NGS) to identify the over or under-representation of genotypes of interest.

In bacteria and yeast, strategies that profit from the efficient homologous recombination in these organisms provide repair templates on the same microarray-synthesized oligonucleotides as the gRNA[19-22]. This enables multiplexed gene-editing in a pooled format with applications for phenotypic profiling of genomic sequence variations.

Because of high throughput, low cost, and broad host versatility, it is interesting to leverage these CRISPR-based methods beyond loss- or gain-of-function screens for the precise

insertion of even longer DNA constructs that deliver reporter molecules or 'tags' to inform about the behavior of the different cellular components encoded in the genome. Rapid access to such collections would synergize with recent developments in image-activated cell sorting (IACS)[23], enabling using the subcellular distribution of a fluorescence signal as criterion for cell sorting.

For the creation of pooled libraries using gene tagging, thousands of DNA constructs must be generated, each containing the reporter gene flanked with the locus-specific homology arms and paired with a corresponding gRNA. However, parallel construction of thousands of such constructs is challenging since no method has been available that could employ microarray-synthesized oligonucleotides for the construction of such resources.

Here, we describe 'CRISPR-assisted tag library engineering' (CASTLING) to create pooled collections of hundreds to thousands of different clones in a single reaction tube. All clones contain the same, large DNA construct (up to several kb in length) accurately inserted at a different, yet precisely specified chromosomal locus. CASTLING is compatible with microarray-based oligonucleotide synthesis since each insertion can be specified by a single oligonucleotide only. CASTLING employs a novel intramolecular recombineering procedure that allows the conversion of such a pool of oligonucleotides into a pool of tagging cassettes.

In this proof-of-concept study, we establish CASTLING in the yeast *Saccharomyces cerevisiae* and explore the power and limitations of the method using gene tagging with fluorescent protein reporters as an example. We derive a set of rules to aid design and selection of effective CRISPR/Cas12a crRNAs for C-terminal tagging of genes in yeast, and determine critical parameters to maximize tagging success in libraries of different sizes. We use a simple assay based on fluorescence-activated cell sorting (FACS) to demonstrate how CASTLING libraries can be used for *ad hoc* characterization of previously uncharacterized proteins, and provide a targeted NGS method for the quantitative analysis of such pooled experiments.

Results

Self-integrating cassettes for CRISPR/Cas12a enhanced gene tagging in yeast

The main component of CASTLING is a linear DNA construct that comprises multiple genetic elements: the 'feature' for genomic integration such as a fluorescent protein tag, a selection marker, a gene for a locus-specific CRISPR RNA (crRNA) for CRISPR/Cas12a (Cpf1)[24] and flanking homology arms to direct the genomic insertion of the DNA fragment by homologous recombination (Fig. 1a). We conceptually termed these DNA constructs 'self-integrating cassettes' (SICs).

We used Cas12a from *Francisella novicida U112* (FnCpf1), which has been reported to be functional in yeast[25], because the genomic target space of the CRISPR/Cas12a endonucleases is defined by A/T-rich protospacer-adjacent motifs (PAMs)[26-29]. This makes them well suited for genetic engineering at transcriptional START and STOP sites not only in yeast but also other organisms (Supplementary Fig. 1).

To test the SIC strategy, we selected several highly-expressed genes in yeast and generated SICs for tagging these genes with a fluorescent protein reporter. After individual transformation of the SICs and selecting clones that had integrated a SIC via the conferred antibiotics resistance, we obtained 100–1,000-times more colonies from hosts that had transiently expressed a Cas12a endonuclease as compared to a host that did not (Fig. 1b). Also, the presence of a crRNA gene specific for the target locus of the SIC was required (Supplementary Fig. 2), indicating that a functional crRNA transcribed from the linear DNA fragment promotes the integration of a SIC. Based on fluorescent colony counts, tagging fidelity had increased from 50–85% in the absence of Cas12a to 95–98% when recombination was stimulated by the action of the Cas12a (Fig. 1b). We also tested CRISPR/Cas12a endonucleases from other species[24] and found that Cas12a from *Acidaminococcus sp. BV3L6* (AsCpf1) showed similar activity as FnCpf1 (Supplementary Fig. 3). To continue, we decided to use FnCpf1 since it offered a broader genomic target space in the yeast genome than AsCpf1 (Supplementary Fig. 4).

Because of the high efficiency of SIC integration, we worried that multiple loci could be tagged within the same cell when different SICs were transformed at the same time. To investigate this, we transformed a mixture of two SICs, one to tag *ENO2* with mCherry and the other one to tag *PDC1* with sfGFP. We detected only few individual colonies where both genes were fluorescently tagged (Fig. 1c), independent of the relative concentration of the two SICs used for transformation (Fig. 1d). Therefore, tagging multiple loci in the same cell would occur rarely if more than one SIC was transformed simultaneously.

Implementing CASTLING for gene tagging in a pooled format

To produce many different SICs in a pooled format using microarray-synthesized oligonucleotides, all gene-specific elements of a SIC, i.e. the crRNA sequence and both homology arms, must be contained in a single oligonucleotide—one for each target locus (Fig. 2a). In turn, this demands for a strategy to convert these oligonucleotides in bulk into the corresponding SICs.

We implemented a three-step molecular recombineering procedure for this conversion (Fig. 2b, Supplementary Fig. 5a–e) that is executed *in vitro*. Its central intermediate is a circular

DNA species formed by the oligonucleotides and a 'feature cassette'. The feature cassette provides all the generic elements of the SIC, i.e. the tag (e.g. GFP), the selection marker and the RNA polymerase III (Pol III) promoter to express the crRNA. The circular intermediates are then amplified by rolling circle amplification (RCA) instead of PCR to avoid the formation of chimeras containing non-matching homology arms. The individual SICs are finally released by cleaving the DNA concatemer using a restriction site in between both homology arms.

To accommodate all gene-specific elements on a single oligonucleotide, it was critical to use a Cas12a endonuclease because its crRNA consists of a comparably short direct repeat sequence (~20 nt) that *precedes* each target-specific CRISPR spacer (~20 nt; Supplementary Fig. 5f). This arrangement allows the Pol III promoter, which drives crRNA expression, to remain part of the feature cassette, while the short Pol III terminator[30] can be included in the oligonucleotide itself. This design leaves enough space for homology arms of sufficient length for homologous recombination (>28 bp[31]). Adding up all the sequences, each oligonucleotide consists of 160–170 nt, which is within the length-limits for oligos synthesized by commercial microarray-based synthesis.

To select CRISPR targets near the desired chromosomal insertion points and to assist the design of the oligonucleotide sequences for microarray synthesis (Supplementary Fig. 6a–d), we wrote the software tool castR (https://github.com/knoplab/castR/). For use with small genomes, castR is available online (http://schapb.zmbh.uni-heidelberg.de/castR/).

CASTLING for a library of nuclear proteins

To test CASTLING, we sought to create a small library covering a set of proteins with known localization[32]. We chose 215 nuclear proteins whose localization had been validated individually in different genome-wide datasets[12,33]. We designed 1,577 oligonucleotides covering all suitable PAM sites within 30 bp around the C-termini of the selected ORFs, yielding 7 oligonucleotides per gene on average. We purchased this oligonucleotide pool three times from different suppliers, one pool from supplier A ('pool A') and two pools from supplier B ('pool B1' and 'B2'; Fig 3a, Online Methods). The amount of starting material for PCR was adjusted to obtain a product within ~20 cycles. We observed that pool A required about 200-fold more starting material than pool B1 or B2 (data not shown). After recombineering with a feature cassette comprising the bright green fluorescent protein reporter mNeonGreen[34], we generated four different libraries in technical duplicates of 50,000–100,000 clones each (Fig. 3a, Supplementary Table 1).

We used NGS in combination with unique molecular identifiers (UMIs)[35] to quantitatively analyze the entire procedure at three stages: After PCR amplification of the oligonucleotide pool and after SIC amplification. To characterize the library, we also used UMIs and combined it with a targeted sequencing method based on Anchor-Seq[12] to analyze in all clones of the libraries the CRISPR spacers of the inserted SICs along with the sequence adjacent to the insertion site.

Overall, the represented oligonucleotide diversity gradually decreased during recombineering (Fig. 3b). Best performance was observed in one duplicate generated from pool B2 that used a high amount of starting material (libraries 4a and 4b), preserving more than 70% of the originally amplified oligonucleotides in the SIC pool and more than 60% of the oligonucleotide diversity in the yeast libraries (Fig. 3b). This loss in complexity was alleviated by the fact that multiple oligonucleotides were included per gene and we observed that more than 90% of desired genotypes were present in library 4a and 4b (Fig. 3c). We noticed that low abundant oligonucleotides after PCR amplification were prone to depletion during SIC preparation, accounting for the observed loss in sequence diversity (Fig. 3d). Across all preparations, copy numbers of individual oligonucleotides were highly correlated between duplicates after PCR (Pearson correlation >0.96), but less between synthesis replicates (0.78–0.90), and least for oligonucleotide pools obtained from different suppliers (Fig. 3e). After recombineering and RCA, no significant correlation of the SIC copy numbers was observed except for libraries 4a and 4b. A more detailed analysis indicated that 50% of the sequences exhibited a copy number change > 2 fold during RCA (Fig. 3f), which could explain the loss of correlation between replicates after RCA. Taken together, these analyses identified the quality and amount of used starting material and recovery during recombineering as critical factors to preserve library diversity. Nevertheless, for a small library of 215 genes, CASTLING enabled tagging most of the selected genes within one library preparation.

Next, we quantified tagging fidelity by fluorescence microscopy, which was possible because we had selected genes encoding proteins with validated nuclear localization. This revealed that 90–95% of the cells had a nuclear localized mNeonGreen signal in all libraries (Fig. 3g–h). The remainder of the cells showed either no fluorescence at all (2–8%, depending on the library) or a fluorescence signal elsewhere, mostly in the cytoplasm (2–6%). So, nearly all genes must have been tagged in the correct reading frame.

For the clones with no fluorescence signal, we suspected either frame-shift mutations in the polypeptide linker (due to faulty oligonucleotides) or in the fluorescent protein reporter (due to limited fidelity of DNA polymerases), or off-target integration of the SIC. Analysis of the Anchor-Seq data identified 280 off-target insertions, corresponding to less than 0.2% of the

clones. Most of these insertions were single occurrences associated with 196 different SICs in total. Only 37 SICs showed off-target insertion at various genomic loci or in more than one library replicate (Fig. 3i). It remains however unclear, which of these insertions were caused by Cas12a-mediated cleavage at an off-target site and which were spontaneous chromosomal insertions.

In addition to these events, we observed fluorescence signals at unexpected subcellular localizations. For example, in library 2b, ~2% of the cells displayed fluorescence at the spindle-pole body, which we could attribute to a Tem1-mNeonGreen gene fusion based on the recorded Anchor-Seq data. Indeed, it turned out that on average 1.6% of all cells across all libraries had integrated SICs originally designed for another experiment in this study, which must have entered SIC or library preparation as a result of contamination.

Together, these experiments demonstrate that in a pooled experiment CASTLING allows for highly efficient tagging of hundreds of genes with low levels of off-target insertion.

Exploring parameters influencing tagging success on a genome-wide scale

Simultaneously with the small pool of nuclear proteins, we designed an oligonucleotide pool for C-terminal tagging of the yeast proteome. For crRNA design, we first retrieved a set of more than 34,000 candidate CRISPR targets by castR using TTV (V = A, C, or G) and TYN (Y = C or T; N = any nucleobase) as protospacer-adjacent motifs (PAMs). Next, we removed sequences that contained thymidine runs longer than five nucleotides, since they may prematurely terminate Pol III transcription[30]. Subsequently, we filtered out crRNA targets with a high off-target estimate and removed most, but not all target sequences that are not destroyed after insertion of the SICs (Supplementary Information). From the remainder, we chose randomly 12,472 sequences (limited by the chosen microarray) that covered 5,664 of 6,681 (85%) of the annotated ORFs in *S. cerevisiae*[36]. Although the number of oligonucleotides per gene was lower as compared to the nuclear pool, the high number of genomic targets should allow to identify parameters that would influence tagging success and clone representation in such large-scale experiments.

After PCR and SIC pool generation, we sequenced the PCR amplicons and one SIC pool. We analyzed the sequencing data with respect to the number of erroneous oligonucleotides by implementing a de-noising strategy to discriminate errors introduced during NGS from errors in the templates[37]. This revealed that the PCR product contained 57% of the designed oligonucleotides, but only 31% of the designed sequences were represented by at least one error-free amplicon. Similarly, 51% of all designed sequences were detected in this SIC pool,

but only 25% were error-free (Fig. 4a). Due to redundancy, the error-free SICs in this pool still covered 45% of the 5,664 ORFs.

To explore how many genes could be tagged with this oligonucleotide pool, we repeated PCR and SIC assembly three times. Following transformation in yeast, this resulted in three independent libraries of 75,000–100,000 clones each. Inspection of the cells by fluorescence microscopy revealed localization across a broad range of sub-cellular compartments (Fig. 4b). By Anchor-Seq, we detected a total of 3,262 different ORFs (58% of all targeted ORFs), of which 1,127 ORFs (20%) were shared across all replicates (Fig. 4c, Supplementary Table 2).

The acquired data allowed us to identify factors that might have impeded efficient genomic integration of a SIC. First, the likelihood of tagging success was 3- to 4-fold decreased when the crRNA target sequence was not disrupted by the inserted SIC, i.e. when recurrent cleavage of the locus was possible. Neither nucleosome occupancy of the PAM, nor of the target sequence itself had a statistically significant impact on the tagging success in this library. However, the choice of the PAM (TTC>TTG>TTA >> TYN) and the first two PAM-proximal nucleotides (CG, CC, GG) increased the chances of target integration 2- to 3-fold each (Fig. 4d, Supplementary Fig. 7a–b). Interestingly, it seemed advantageous to target genes on their non-transcribed strand by CRISPR/Cas12a. Despite the limited success to create a genome-wide library at first trial, we anticipated that these parameters could help to improve tagging success for CASTLING in yeast.

CASTLING of large libraries

To further investigate the creation of genome-wide pooled libraries with CASTLING, we designed a new microarray for tagging 5,940 ORFs. Applying these rules for each ORF, we selected 17,691 target sites near the STOP codon and filled up the remaining positions on a 27,000-well array. We generated three libraries in total using two different strategies to investigate the minimal effort that would be required for creating a large library with CASTLING.

First, we pooled SICs from 30 RCAs and generated a total of 748,000 clones, which we divided into a large library of 704,000 clones (LibA), and a small library of 44,000 clones (LibB). Second, we constructed a third library of 116,000 clones (LibC) using a SIC pool made from two RCAs of the same oligonucleotide pool (Fig. 5a). To quantify genotype composition in each of the different libraries, we again used Anchor-Seq at the crRNA junction in combination with UMIs. Taken together, the three libraries contained tagged alleles of 76% of all the targeted ORFs with an overlap of 43% between the three libraries

(Fig. 5b–c). The largest library, LibA, contained the highest number of tagged ORFs, namely 3,801 ORFs, corresponding to 64% of the design. Interestingly, the much smaller library LibB with 44,000 clones already contained 80% of these genotypes. LibB and LibC each covered ~50% of the desired ORFs, with an overlap in 2,038 of the genes. In practical terms, this implied that about one third of the intended genes could be reliably and reproducibly obtained with minimal effort by recovering about 40,000–120,000 clones only.

We validated the rule set used for oligo design by comparing SICs with approximately equal copy number in the SIC pool (Supplementary Figure 8a–b).

Functional studies that use pooled libraries essentially depend on enrichment procedures to physically separate cells based on the information provided by the reporter. When using fluorescent protein fusions to endogenous proteins, high-resolution fluorescence images of the cells would be the method of choice, as this would enable scoring and subsequent sorting based on very complex and informative phenotypes. The necessary technology is currently under development[23]. To showcase however, that libraries created by CASTLING can be used in such profiling studies, we reverted to fluorescence-activated cell sorting (FACS) which permits sorting of cell based on fluorescence brightness.

We first isolated the subpopulation of cells that exhibited sufficient fluorescence for detection by FACS fluorescent cells from a library by FACS and subsequently sorted this population into fractions of cells with increasing brightness (Fig. 5d). The cells in each fraction were analyzed by Anchor-Seq using on-site Oxford Nanopore sequencing on a MinION device as a means for *ad hoc* identification of the most prominently represented genes in the sorted populations. This experiment also identified eight ORFs that had never been characterized before in terms of protein abundance in other genome-scale experiments. Subsequent gene-wise tagging confirmed that the encoded proteins were expressed with the expected brightness (Fig. 5e, Supplementary Table 3). This outlines not only a rapid workflow for pooled profiling experiments, but also suggests that non-exhaustive libraries offer an opportunity to identify and/or characterize novel genotypes of interest.

Taken together, these results establish CASTLING as a rapid method to tag a large fraction of the yeast genes with a fluorescent protein reporter in a one-pot experiment.

Discussion

We developed CASTLING to enable the rapid creation of pooled libraries of clones with large chromosomal insertions such as fluorescent protein tags.

Typically, libraries in yeast have been constructed gene-wise in an arrayed format using PCR-targeting[38]. Based on our own experience[12,39], the construction of arrayed libraries depends on special equipment for parallelization of the procedures, it requires a (costly) resource of arrayed primers for PCR tagging, and the workload for handling thousands of strains keeps multiple researchers busy for several months.

In contrast, much less resources must be committed to the creation of a library by CASTLING. All the necessary oligonucleotides can be obtained from microarrays, which are about two orders of magnitude cheaper than a genome-wide set of conventional column-purified oligonucleotides. Once an established oligonucleotide pool is available, it can be reused to construct a variety of SIC pools containing different features, i.e. tags or selection markers. The construction of SIC pools is rapid and can be completed within 1-2 days since the CASTLING workflow avoids preparatory sub-cloning into a plasmid library, which is commonly used in other multiplexed gene-editing approaches[19-21,40]. Transformation and growth of the yeast clones take another 2–3 days, followed by recovery and analysis of the library. This makes library preparation by CASTLING very efficient and therefore it is possible to create a new library for each strain background or mutant of interest. Classical libraries, in contrast, are confined to the background they were made in and require genetic crossing to introduce a mutant, which depends on strains specifically constructed for these procedures[41].

In addition to the versatility and flexibility of library creation, tagging fidelity by CASTLING is above 90%, vastly exceeding the fidelity observed in conventional gene tagging by PCR-targeting, where routinely 50–85% of the obtained clones are correct. It may be worth mentioning that elimination of the false clones during the construction of classical arrayed libraries remains one of the most laborious steps. With CASTLING, ‘false clones’ cannot obstruct the correct interpretation of a screening because Anchor-Seq can analyze, verify, and quantify all genotypes available at the beginning of an experiment as well as their respective enrichment or depletion after phenotypic selection. This allows excluding faulty genotypes while completing the analysis, which is typically not possible in other multiplexed CRISPR-based gene editing approaches which rely on indirect measures for genotype determination.

A potential down-side of CASTLING and many other pooled library approaches lies within the initial indeterminacy of the exact library composition: Each transformation will yield a slightly different pool composition.

Currently, genotype coverage with CASTLING can exceed 90% when relatively small libraries with hundreds of genes are created and reproducibly reached 50% for libraries with thousands of genes using only ~10-fold oversampling. We have identified that SICs for

which the CRISPR target site would be destroyed after integration, or SICs that had a GC-rich crRNA in its PAM-proximal dinucleotides, yielded higher clone numbers as compared to SICs lacking those features (Supplementary Fig. 8).

The identified parameters increased the likelihood of tagging success, but they might also displace the number of clones for which only less efficient SICs could be designed, so that additional oversampling would be required in this case. Along this line, a better strategy to increase coverage might be to use successive rounds of CASTLING involving each time a new microarray to target the remainder of the genes. The first array would target the ~30% of genes that can be reproducibly tagged in any approach (Fig. 5), while subsequent arrays would incrementally complete the library with almost proportional scaling efforts in terms of clones to be collected. Probably, it would require 2-4 rounds of CASTLING with a total of 60,000–120,000 clones to tag >60–90% of all 5,500–6,000 genes in yeast. This would exceed available genome-wide tagging collection, e.g. the GFP collection with 4,159 ORFs (Thermo Fisher), the TAP-tag collection with 4,247 ORFs (Dharmacon) or our tandem fluorescent timer collection with 4,081 ORFs[39]. Importantly, such an optimization might be necessary only once; afterwards, all oligonucleotide pools could be used in parallel to generate a nearly complete library. This approach might also yield optimized rule sets to guide the development of CASTLING for a different species.

Despite this possibility, a major factor that operated on the decrease in tagging success seemed to be oligonucleotide quality. We have sequenced and thoroughly analyzed one of the oligonucleotide pools for large library creation. Only a fraction of the designed sequences was represented by full-length perfect oligonucleotides. Indeed, error-free synthesis of long oligonucleotides remains challenging[42,43]. To increase the chance of representing each target locus by a perfect oligonucleotide, it might be beneficial to use as many different oligonucleotides per gene as possible or to include multiple redundant sequences (depending on the size of the microarray) if an adequate SIC design for a specific locus is known.

It is important to stress that faulty oligonucleotides do *not* impact the fidelity of the tagging. This is impressively demonstrated with the nuclear protein libraries that were prepared with three different oligonucleotide pools, all of which showing >90% in-frame tagging rates (Fig. 3). This may be either because faulty oligonucleotides fail to assemble with the feature cassette or because errors in their crRNA and/or the homology arms render the SIC inactive due to reduced recombination frequencies[44]. This results in an intrinsic ‘quality control’ during CASTLING yielding correctly tagged genes in the majority.

Prospective applications of CASTLING

In combination, CASTLING and quantitative Anchor-Seq enable the rapid creation and analysis of pooled libraries with tagged genes respectively. Since each reaction tube can contain an entire library, the pooled format is able to address much broader, comparative questions, including different genetic backgrounds and/or environmental conditions. In which way pooled tag libraries will be useful for molecular, cell, or genome biology research will depend on procedures that provide the necessary throughput for profiling and physical sorting individual cells based on a suitable phenotypic read-out. Our simple FACS enrichment experiment can serve as proof of principle in this regard as current flow cytometry-based cell sorters cannot resolve more complex cellular phenotypes such as the subcellular localization of proteins[45]. Therefore, the recent development of an image-activated cell sorting (IACS) instrument[23] can be considered a breakthrough to study e.g. how the localization of thousands of proteins is changed under different conditions. We think that for such methods, CASTLING constitutes an important development enabling a variety of entirely new experimental designs and analyses, ranging from functional genomics to biomedical research, paving the way to a new paradigm of shot-gun cell biology.

Beyond yeast, CASTLING could be adapted for other organisms able to repair DNA lesions by homologous recombination, including bacteria, fungi, flies and worms, and potentially also in plants and mammalian cells. First evidence that this is the case is provided in Fueller et al. (pre-print, https://doi.org/10.1101/473876) where we show that an adapted SIC strategy can be used for efficient endogenous tagging of genes in mammalian cells.

Please note: Inadequate adoption of CASTLING can unwittingly generate clones qualified to initiate a gene-drive upon sexual reproduction[46]. This can be easily prevented (Supplementary Information).

Competing financial interest statement. The authors declare no competing financial interests.

Author contribution. M.K. conceived the project. M.K., B.C.B., K.H. and M.M. designed the experiments and B.C.B., K.H., M.M., and D.K. performed the experiments. E.L. and U.S. contributed methods. K.H., B.C.B., M.K., and M.M. analyzed the data. M.K. and B.C.B. wrote the manuscript. All authors read and approved the final manuscript.

Acknowledgements. The authors wish to thank Ilia Kats, Cyril Mongis, and Krisztina Gubicza for help with IT infrastructure and experiments. We acknowledge support by the Deutsche Forschungsgemeinschaft (DFG KN498/12-1), the state of Baden-Württemberg through bwHPC for high-performance computing and SDS@hd for data storage (grant INST

35/1314-1 FUGG) and the Dietmar Hopp foundation. K.H. is supported by a HBIGS graduate school fellowship. We also acknowledge help from the Flow Cytometry Core Facility at ZMBH, and the Deep Sequencing Core Facility of the University of Heidelberg, both of which are supported by the CellNetworks cluster of excellence.

References.

1. Sopko, R. *et al.* Mapping pathways and phenotypes by systematic gene overexpression. *Mol Cell* **21,** 319–330 (2006).
2. Douglas, A. C. *et al.* Functional analysis with a barcoder yeast gene overexpression system. *G3* **2,** 1279–1289 (2012).
3. Kuzmin, E. *et al.* Systematic analysis of complex genetic interactions. *Science* **360,** eaao1729 (2018).
4. Ghaemmaghami, S. *et al.* Global analysis of protein expression in yeast. *Nature* **425,** 737–741 (2003).
5. Hu, C.-D., Chinenov, Y. & Kerppola, T. K. Visualization of interactions among bZIP and Rel family proteins in living cells using bimolecular fluorescence complementation. *Mol Cell* **9,** 789–798 (2002).
6. Belle, A., Tanay, A., Bitincka, L., Shamir, R. & O'Shea, E. K. Quantification of protein half-lives in the budding yeast proteome. *Proc Natl Acad Sci USA* **103,** 13004–13009 (2006).
7. Khmelinskii, A. *et al.* Tandem fluorescent protein timers for in vivo analysis of protein dynamics. *Nat Biotechnol* **30,** 708–714 (2012).
8. Gavin, A.-C. *et al.* Functional organization of the yeast proteome by systematic analysis of protein complexes. *Nature* **415,** 141–147 (2002).
9. Krogan, N. J. *et al.* Global landscape of protein complexes in the yeast Saccharomyces cerevisiae. *Nature* **440,** 637–643 (2006).
10. Tarassov, K. *et al.* An in vivo map of the yeast protein interactome. *Science* **320,** 1465–1470 (2008).
11. Yofe, I. *et al.* One library to make them all: streamlining the creation of yeast libraries via a SWAp-Tag strategy. *Nature Methods* **13,** 371–378 (2016).
12. Meurer, M. *et al.* Genome-wide C-SWAT library for high-throughput yeast genome tagging. *Nature Methods* **15,** 598–600 (2018).
13. Winston, F., Dollard, C. & Ricupero-Hovasse, S. L. Construction of a set of convenient Saccharomyces cerevisiae strains that are isogenic to S288C. *Yeast* **11,** 53–55 (1995).
14. Wilkening, S. *et al.* Genotyping 1000 yeast strains by next-generation sequencing. *BMC Genomics* **14,** 90 (2013).
15. Roemer, T., Davies, J., Giaever, G. & Nislow, C. Bugs, drugs and chemical genomics. *Nature Publishing Group* **8,** 46–56 (2011).
16. Shalem, O. *et al.* Genome-scale CRISPR-Cas9 knockout screening in human cells. *Science* **343,** 84–87 (2014).
17. Zhou, Y. *et al.* High-throughput screening of a CRISPR/Cas9 library for functional genomics in human cells. *Nature* **509,** 487–491 (2014).

18. Kuscu, C. *et al.* CRISPR-STOP: gene silencing through base-editing-induced nonsense mutations. *Nature Methods* **14,** 710–712 (2017).
19. Garst, A. D. *et al.* Genome-wide mapping of mutations at single-nucleotide resolution for protein, metabolic and genome engineering. *Nat Biotechnol* **35,** 48–55 (2017).
20. Sadhu, M. J. *et al.* Highly parallel genome variant engineering with CRISPR-Cas9. *Nat. Genet.* **50,** 510–514 (2018).
21. Roy, K. R. *et al.* Multiplexed precision genome editing with trackable genomic barcodes in yeast. *Nat Biotechnol* **36,** 512–520 (2018).
22. Guo, X. *et al.* High-throughput creation and functional profiling of DNA sequence variant libraries using CRISPR–Cas9 in yeast. *Nat Biotechnol* **36,** 540–546 (2018).
23. Nitta, N. *et al.* Intelligent Image-Activated Cell Sorting. *Cell* **175,** 266–276.e13 (2018).
24. Zetsche, B. *et al.* Cpf1 is a single RNA-guided endonuclease of a class 2 CRISPR-Cas system. *Cell* **163,** 759–771 (2015).
25. Verwaal, R., Buiting-Wiessenhaan, N., Dalhuijsen, S. & Roubos, J. A. CRISPR/Cpf1 enables fast and simple genome editing of Saccharomyces cerevisiae. *Yeast* (2017). doi:10.1002/yea.3278
26. Zhang, L., Kasif, S., Cantor, C. R. & Broude, N. E. GC/AT-content spikes as genomic punctuation marks. *Proc Natl Acad Sci USA* **101,** 16855–16860 (2004).
27. Kim, H. K. *et al.* In vivo high-throughput profiling of CRISPR-Cpf1 activity. *Nature Methods* **14,** 153–159 (2017).
28. Tu, M. *et al.* A 'new lease of life': FnCpf1 possesses DNA cleavage activity for genome editing in human cells. *Nucl Acids Res* **45,** 11295–11304 (2017).
29. Swiat, M. A. *et al.* FnCpf1: a novel and efficient genome editing tool for Saccharomyces cerevisiae. *Nucl Acids Res* **45**, 12585–12598 (2017).
30. Arimbasseri, A. G., Rijal, K. & Maraia, R. J. Transcription termination by the eukaryotic RNA polymerase III. *Biochimica et Biophysica Acta (BBA) - Gene Regulatory Mechanisms* **1829,** 318–330 (2013).
31. Orr-Weaver, T. L., Szostak, J. W. & Rothstein, R. J. Yeast transformation: a model system for the study of recombination. *Proc Natl Acad Sci USA* **78,** 6354–6358 (1981).
32. Huh, W.-K. *et al.* Global analysis of protein localization in budding yeast. *Nature* **425,** 686–691 (2003).
33. Dubreuil, B. *et al.* YeastRGB: comparing the abundance and localization of yeast proteins across cells and libraries. *Nucl Acids Res* **425,** 737 (2018).
34. Shaner, N. C. *et al.* A bright monomeric green fluorescent protein derived from Branchiostoma lanceolatum. *Nature Methods* **10,** 407–409 (2013).
35. Kivioja, T. *et al.* Counting absolute numbers of molecules using unique molecular identifiers. *Nature Methods* **9,** 72–74 (2011).
36. Engel, S. R. *et al.* The reference genome sequence of Saccharomyces cerevisiae: then and now. *G3* **4,** 389–398 (2014).
37. Callahan, B. J. *et al.* DADA2: High-resolution sample inference from Illumina amplicon data. *Nature Methods* **13,** 581–583 (2016).
38. Baudin, A., Ozier-Kalogeropoulos, O., Denouel, A., Lacroute, F. & Cullin, C. A simple and efficient method for direct gene deletion in Saccharomyces cerevisiae. *Nucl Acids Res* **21,** 3329–3330 (1993).
39. Khmelinskii, A. *et al.* Protein quality control at the inner nuclear membrane. *Nature* **516,** 410–413 (2014).
40. Billon, P. *et al.* CRISPR-Mediated Base Editing Enables Efficient Disruption of

Eukaryotic Genes through Induction of STOP Codons. *Mol Cell* **67,** 1068–1079.e4 (2017).

41. Tong, A. H. *et al.* Systematic genetic analysis with ordered arrays of yeast deletion mutants. *Science* **294,** 2364–2368 (2001).
42. Kosuri, S. & Church, G. M. Large-scale de novo DNA synthesis: technologies and applications. *Nature Methods* **11,** 499–507 (2014).
43. Klein, J. C. *et al.* Multiplex pairwise assembly of array-derived DNA oligonucleotides. *Nucl Acids Res* **44,** e43–e43 (2016).
44. Anand, R., Beach, A., Li, K. & Haber, J. Rad51-mediated double-strand break repair and mismatch correction of divergent substrates. *Nature* **544,** 377–380 (2017).
45. Barteneva, N. S., Fasler-Kan, E. & Vorobjev, I. A. Imaging flow cytometry: coping with heterogeneity in biological systems. *J. Histochem. Cytochem.* **60,** 723–733 (2012).
46. Reaume, S. E. & Tatum, E. L. Spontaneous and nitrogen mustard-induced nutritional deficiencies in Saccharomyces cerevisiae. *Arch Biochem* **22,** 331–338 (1949).
47. Ho, B., Baryshnikova, A. & Brown, G. W. Unification of Protein Abundance Datasets Yields a Quantitative *Saccharomyces cerevisiae* Proteome. *Cell Syst.* **6**, 192-205.e3 (2018).

Figures and Legends

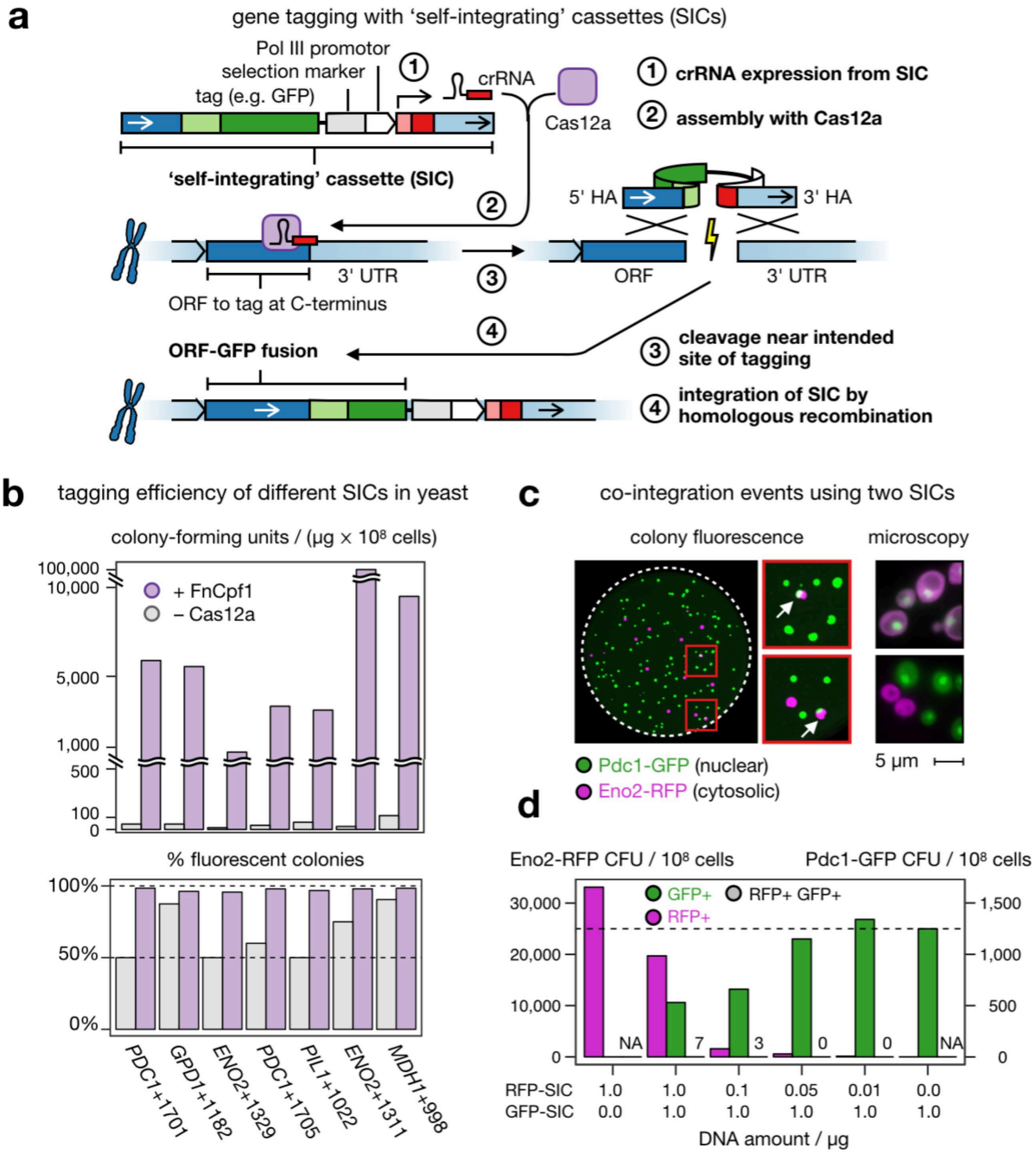

Figure 1 | CRISPR/Cas12a-assisted gene-tagging with 'self-integrating cassettes' (SICs) in yeast. (**a**) After transformation of the SIC into a cell, the crRNA expressed from the SIC directs a CRISPR/Cas12a endonuclease to the genomic target locus where the DNA double-strand is cleaved. The lesion is repaired by homologous recombination using the SIC as repair template so that an in-frame gene fusion is observed. (**b**) Efficiency of seven SICs of C-terminal tagging of highly expressed open-reading frames (ORFs) with a fluorescent protein reporter, in the absence (grey) or presence (purple) of FnCpf1. Colony-forming units per microgram of DNA and integration fidelity by colony fluorescence are shown. (**c**) Co-

integration events upon simultaneous transformation of two SICs directed against either *ENO2* or *PDC1*. Both SICs confer resistance to Geneticin (G-418), but contain different fluorescent protein tags. Colonies exhibiting green and red fluorescence (arrows) were streaked to identify true co-integrands. False-color fluorescence microscopy images show nuclear Pdc1-GFP in green and the cytosolic Eno2-RFP in magenta. (**d**) Titration of both SICs against each other (lower panel) with evaluation of GFP-tagged (GFP+), RFP-tagged (RFP+) or co-transformed (GFP+RFP+) colonies.

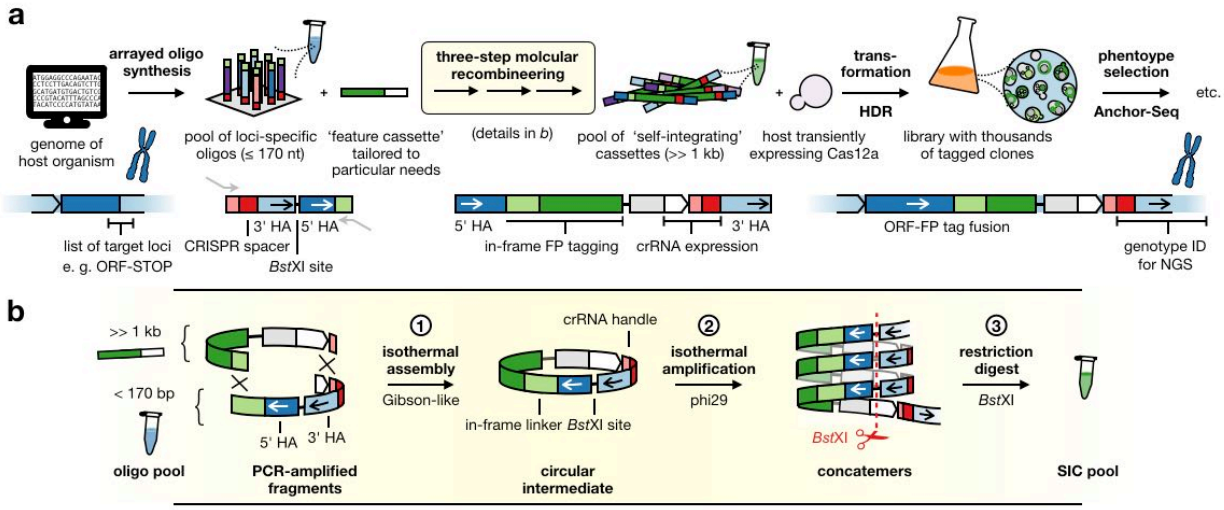

Figure 2 | CASTLING in a nutshell. (**a**) For each target locus, a DNA oligonucleotide with site-specific homology arms (HA) and a CRISPR spacer encoding a target-specific crRNA is designed and synthesized as part of an oligonucleotide array. The resulting oligonucleotide pool is recombineered with a custom-tailored feature cassette into a pool of 'self-integrating cassettes' (SICs). This results in a clone collection (library) that can be subjected to phenotypic screening and genotyping, e.g. using Anchor-Seq[12]. (**b**) The three-step recombineering procedure for SIC pool generation; details in the main text and Online Methods.

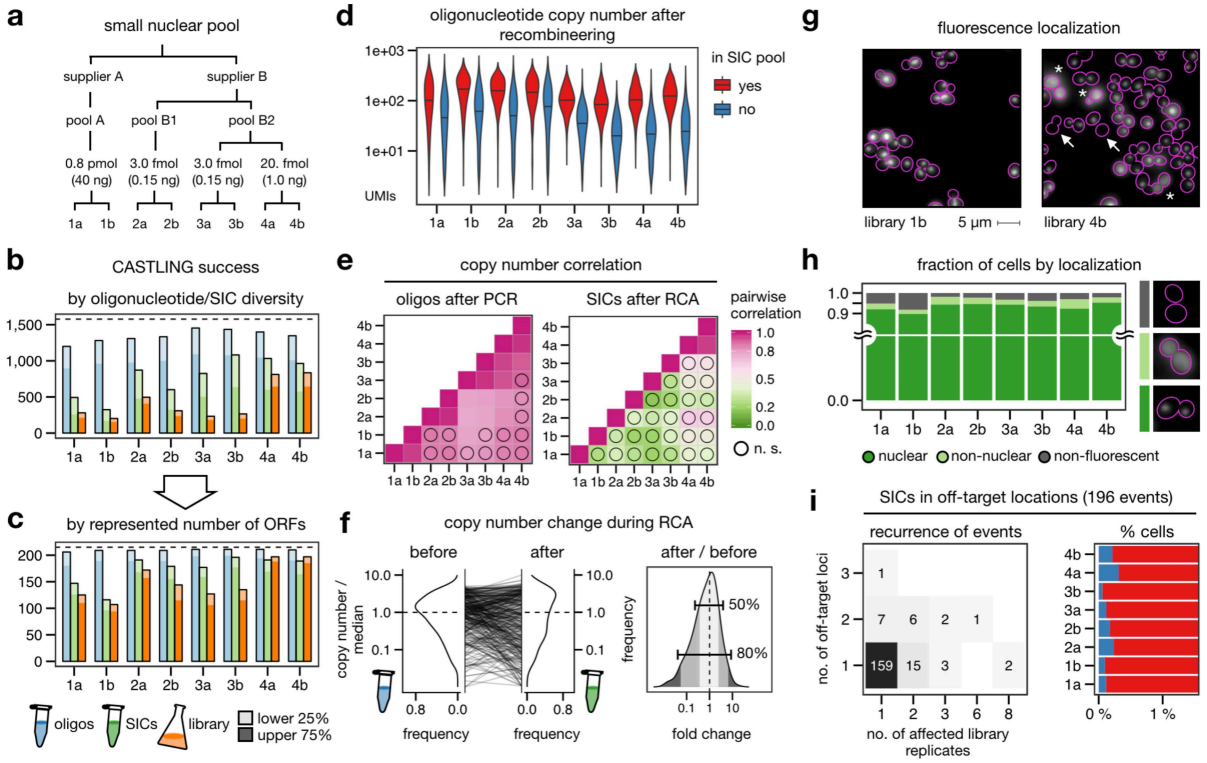

Figure 3 | CASTLING for tagging 215 nuclear proteins with a green fluorescent protein. (**a**) Three oligonucleotide pools of the same design (1,577 sequences) were used to create four tag libraries by CASTLING in duplicate sampling the indicated amount of starting material for PCR. (**b**) Detected oligonucleotide sequences of the design after PCR amplification (blue), 'self-integrating' cassette (SIC) assembly (green) and in the final library (orange); oligonucleotides with copy number estimates (unique UMI counts) in the lowest quartile (lower 25%) are shown in light shade. (**c**) Same as (b), but evaluated in terms of open reading frames (ORFs) represented by the oligonucleotides or SICs. (**d**) Copy number of PCR amplicons recovered (red) or lost (blue) after recombineering; black horizontal lines indicate median UMI counts. (**e**) Pairwise correlation of oligonucleotide or SIC copy number between replicates after PCR or rolling-circle amplification (RCA) respectively; n.s., not significant ($p > 0.05$). (**f**) Kernel density estimates of copy number frequency in replicate 4a as normalized to the median copy number observed in the oligonucleotide pool (before recombineering) and after recombineering into the SIC pool (left panel); the distribution of fold-changes (right panel) highlights two frequency ranges: [0.1–0.9], i.e. 80% of SICs, and [0.25–0.75], i.e. 50% of SICs. (**g**) Representative fluorescence microscopy images of cells displaying nuclear, diffuse non-nuclear (asterisks), or no mNeonGreen fluorescence (arrows). (**h**) Quantification of fluorescence localization in >1,000 cells in each replicate. (**i**) Recurrence of off-target events as revealed by Anchor-Seq across all library replicates and all genomic loci (left panel); the fraction of cells with SICs integrated at off-target sites (blue) within each clone population (red) is shown (right panel, axis trimmed).

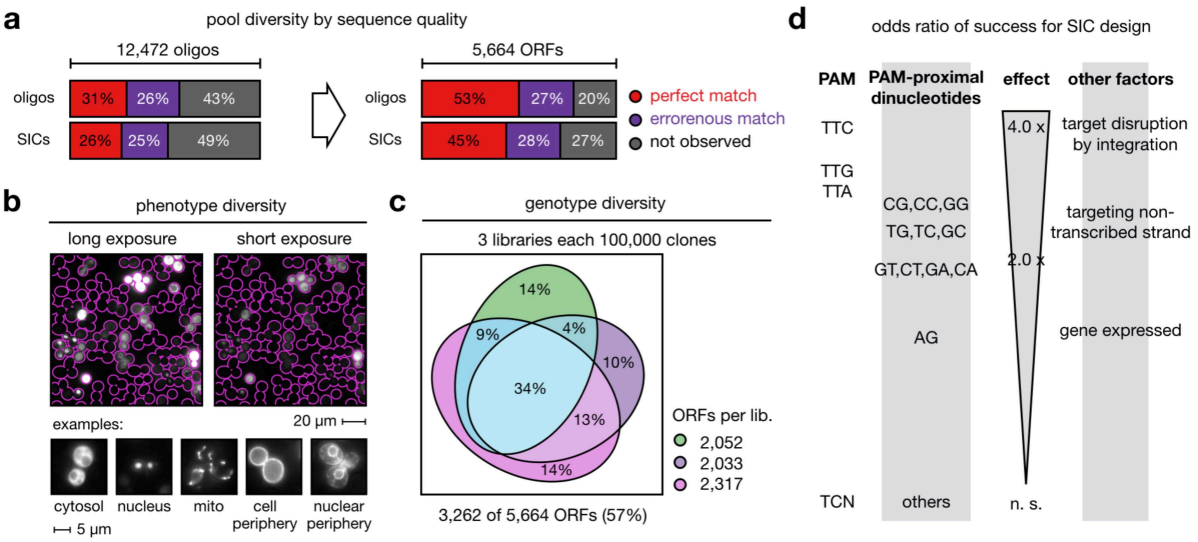

Figure 4 | Identification of factors influencing clone representation in CASTLING. (**a**) Sequence quality of an oligonucleotide pool after PCR amplification and SIC assembly. Following de-noising of NGS artifacts, molecules that aligned with any of the 12,472 designed oligonucleotides were classified error-free, erroneous or absent at the respective stage (left panel). The genotype space (designed: 5,664 ORFs) covered by each class (right panel). (**b**) Representative fluorescence microscopy images of a pooled tag library. (**c**) Genotype diversity within three independent library preparations (100,000 clones each) generated from the same oligonucleotide pool; all libraries combined tagged 3,262 different ORFs. (**d**) Summary of parameters significantly ($p < 0.05$) increasing the likeliness of tagging success beyond SIC abundance (details in Supplementary Fig. 7a–b).

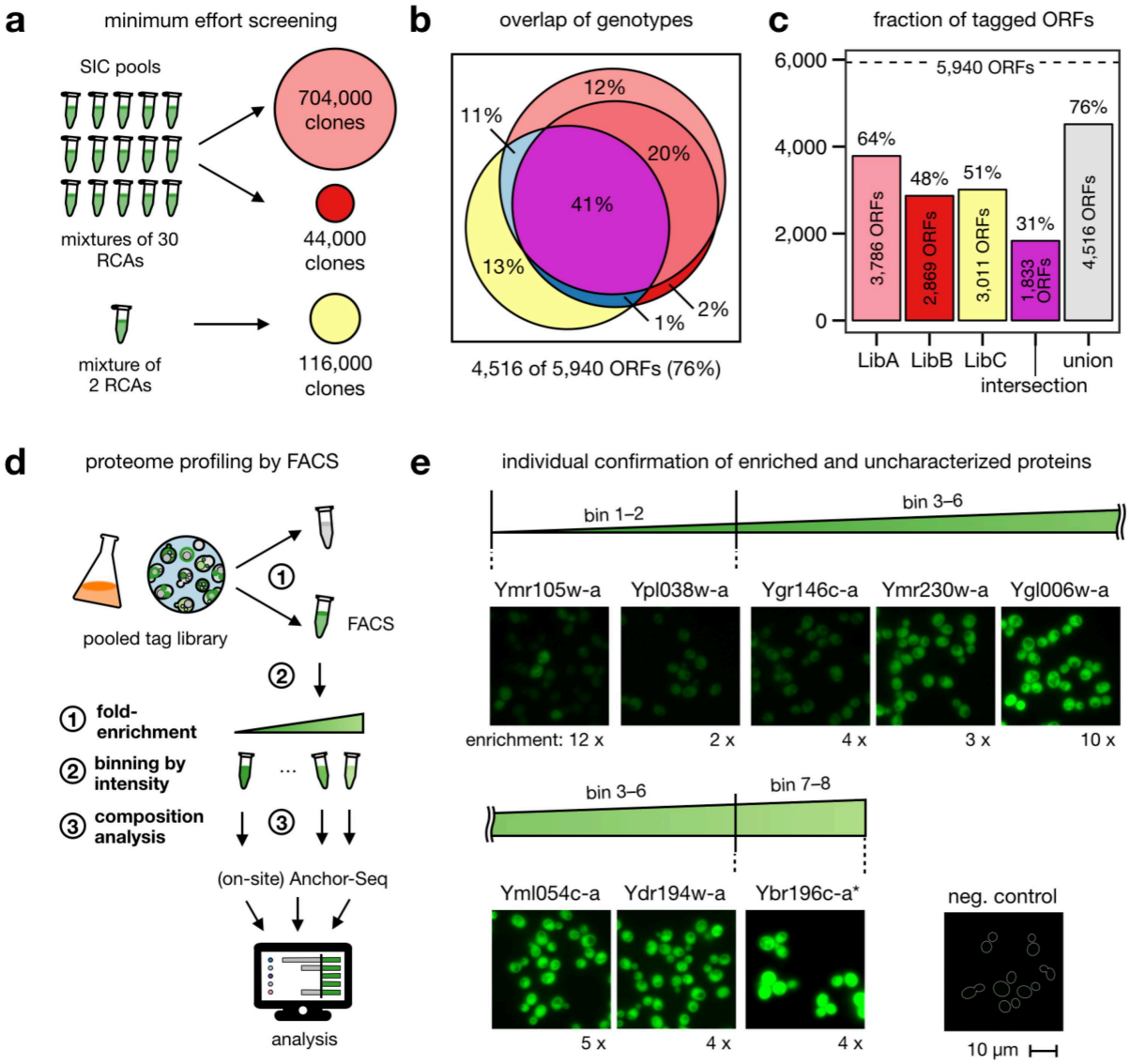

Figure 5 | Approaching proteome-wide coverage. (**a**) Three libraries with different numbers of collected clones were generated from SIC pools combining either 2 or 30 recombineering reactions to investigate the minimum effort for a proteome-wide (design: 5,940 ORFs) CASTLING library (details in Materials and Methods). (**b**) Venn diagram of genotypes recovered in each of the three libraries; all libraries combined tagged 4,516 different ORFs. (**c**) Genotype diversity in each of the three libraries, shared between them, or after their combination. (**d**) Proteome profiling by fluorescence intensity of a non-exhaustive mNeonGreen tag library with 100,000 clones (2,052 different ORFs) using FACS. After enriching the fluorescent sub-population of the library and determining the fold-enrichment of each genotype by NGS, this sub-population was sorted into eight bins according to fluorescent intensity. Analysis of each bin by Anchor-Seq and on-site Oxford nanopore sequencing allowed the assignment of an expected protein abundance for each genotype. (**e**) Eight enriched genotypes that had not been characterized in other genome-

scale experiments[47] were tagged manually to verify whether fluorescence intensity corresponded with their predicted characterization by FACS. Same exposure time for all fluorescent microscopy images; Ybr196c-a was imaged at 10% excitation.

Online Methods.

Yeast strains and plasmids. All strains were derived from ESM356-1 (*Saccharomyces cerevisiae* S288C, *MAT***a** *ura3*-52 *leu2*Δ1 *his3*Δ200 *trp1*Δ63, which is a spore from strain FY1679[1,2]) and are listed in Supplementary Table 4. Plasmids are listed in Supplementary Table 5. Human codon-optimized Cas12a (Cpf1)-family proteins[3] of *Francisella novicida U112* (FnCpf1), *Lachnospiriceae bacterium ND2006* (LbCpf1), *Acidaminococcus sp. BV3L6* (AsCpf1), and *Moraxella bovoculi 237* (MbCpf1) were expressed using either the galactose-inducible *GAL1* promoter[4] from plasmids integrated into the *ura3*-52 locus (pMaM486, pMaM487, pMaM488, pMaM489), or expressed from the constitutive *TEF1* promoter using a low-copy centromeric plasmid as a backbone (pBeB503, pBeB603, pBeB703, pBeB803). Yeast growth, cell lysis and Western blot detection of HA tagged proteins were as described[5].

CASTLING library design. To facilitate oligonucleotide design, an *R* package is available from our repository (https://github.com/knoplab/castR) that ships along with a GUI. For small genomes, the GUI can be accessed online (http://schapb.zmbh.uni-heidelberg.de/users/knoplab/castR/). The principles used for oligo design are described in Supplementary Note 1.

Oligonucleotide sequences used in this study are given in Supplementary Table 7 (Fig. 3), Supplementary Table 8 (Fig. 4), and Supplementary Table 9 (Fig. 5).

Generation of 'self-integrating' cassettes (SICs) for individual genes. Individual SICs were generated by PCR using a corresponding plasmid template (Supplementary Table 5) and using primers (Supplementary Table 9) that introduced the required 5' and 3' homology arms along with a locus-specific crRNA spacer. Cycling conditions for VELOCITY DNA polymerase-based amplification (Bioline) were 97 °C for 3 min, followed by 30 cycles of 97 °C (30 sec), 63 °C (30 sec), 72 °C (2 min 30 sec) and a final 72 °C (5 min) extension hold. The reactions were column-purified and adjusted to equal SIC concentration before transformation.

Recombineering procedure to construct SIC pools for CASTLING. *Amplification of oligonucleotide pool and feature cassettes*: The oligonucleotide pools used in this study (Supplementary Table 10) were synthesized by either CustomArray Inc. (pool P1A and P2), Twist Bioscience (pool P1B and P1C), or Agilent Technologies (pool P3), and resuspended in TE. Pool dilution and annealing temperature were optimized in each case to yield a uniform product of the expected length (Supplementary Fig. 5a, Supplementary Table 1–2). In this study, pool P2 was diluted 1,000-fold and 1.5 fmol were amplified using VELOCITY DNA polymerase (Bioline) with forward primer pool-FP1 and reverse primer pool-RP2 using

the following PCR conditions: 97 °C for 3 min, followed by 20 cycles of 97 °C (30 sec), 58 °C (30 sec), 72 °C (20 sec), and a final 72 °C (5 min) extension hold. To keep library member representation as uniform as possible, using more input material and higher annealing temperatures is desirable, as this will usually require fewer PCR cycles for amplification of the full-length synthesis product. All other pools were designed to allow for amplification in 15 cycles using Herculase II DNA polymerase (Agilent Technologies) with forward primer pool-FP2 (or pool-FP3, as indicated) and reverse primers pool-RP2 (or pool-RP3). Cycling conditions were: 95 °C for 2 min, followed by 6 cycles of 95 °C (20 sec), touch-down from 67 °C (20 sec, $\Delta T = -1$ °C per cycle), 75 °C (30 sec), then 9 cycles of 95 °C (20 sec), 67 °C (20 sec), 72 °C (30 sec), and a final 72 °C (5 min) extension hold. Primers and truncated oligonucleotides (< 75 bp) were removed using NucleoSpin Gel and PCR clean-up columns (MACHERY-NAGEL GmbH & Co. KG). Feature cassettes were amplified by PCR using cognate cassette-FP and cassette-RP and any compatible plasmid template (50 ng, Supplementary Table 5) under the following conditions: 97 °C for 3 min, followed by 30 cycles of 97 °C (30 sec), 63 °C (30 sec), 72 °C (2 min 30 sec) and a final 72 °C (5 min) extension hold. The reaction was treated with *Dpn*I (New England Biolabs) *in situ* and cleaned-up using NucleoSpin Gel and PCR clean-up columns. For PCR, VELOCITY high-fidelity DNA polymerase (Bioline) was used with the manufacturer's reaction mix supplemented with 500 µM betaine (Sigma-Aldrich). For analysis, 2 µL of the reaction were used for DNA gel electrophoresis (0.8% agarose, Supplementary Fig. 5a).

Recombineering step 1: Circularization of the amplified oligonucleotide pool (0.8 pmol) with the amplified feature-cassette (0.2 pmol) was performed using NEBuilder HiFi DNA Assembly Master Mix (New England Biolabs) in a total reaction volume of 20 µL at 50 °C for 30 min. For analysis by DNA gel electrophoreses, 10 µL of the reaction were used (0.8% agarose, Supplementary Fig. 5b).

Recombineering step 2: To amplify selectively the circular product from Step 1, rolling circle amplification was used. First, the annealing mixture was set up (total volume: 5 µL in a PCR tube) using 1 µL of the crude circularization reaction, 2 µL exonuclease-resistant random heptamers (500 µM, Thermo Fisher Scientific), 1 µL of annealing buffer (stock: 400 mM Tris-HCl, 50 mM $MgCl_2$, pH = 8.0) and 1 µL of water. For annealing, the mixture was heated to 94 °C for 3 min and cooled down in thermocycler at 0.5 °C/sec to 4 °C. Then, 15 µL amplification mixture were added (consisting of 2.0 µL 10 x phi29 reaction buffer, 2.0 µL 100 mM dNTP mix, 0.2 µL 100 x BSA, 10 mg/mL, and 0.6 µL phi29 DNA-polymerase; all from New England Biolabs). Amplification was allowed to proceed for 12–18 h at 30 °C, followed by heat-inactivation of the enzymes at 80 °C for 10 min. For analysis by DNA gel electrophoresis (0.8% agarose) 0.5 µL of this reaction was used (Supplementary Fig. 5c).

Recombineering step 3: To release the SICs, 20 U of the restriction enzyme *Bst*XI (New England Biolabs) were added directly to the amplification reaction and the mixture was incubated for 3 hours at 37 °C. Typically, such a reaction yielded 10–20 µg of SICs. For DNA gel electrophoresis, 1 µL was used (Supplementary Fig. 5d).

Estimation of recombineering fidelity in libraries shown in Fig. 3 and Fig. 5: The oligonucleotide pools were analysed by NGS after PCR amplification and after recombineering including unique molecular identifiers (UMIs) for de-duplication. For the PCR amplicons, fragments with UMIs were generated using 200 ng starting material (purified by ethanol precipitation) in 2 cycles of PCR with Herculase II Fusion DNA Polymerase (Agilent Technologies) using an equimolar mixture of P023poolseqNN-primers (1 mM final concentration) in a 25 µL reaction. Cycling conditions were based on the manufactures recommendations (62 °C annealing, 30 sec elongation). The reactions were purified with NucleoSpin Gel and PCR clean-up columns using diluted NTI buffer (1:5 in water) to facilitate primer depletion, and the fragments eluted in 20 µL 5 mM Tris-HCl (pH = 8.5) each. To remove residual primers, 7 µL of eluate were treated with 0.5 µL exonuclease I (*E. coli*, New England Biolabs) in 1 x Herculase II reaction buffer (1 h, 37 °C) and heat-inactivated (20 min, 80 °C). The reaction was used without further purification as input for a second PCR (Herculase II Fusion DNA Polymerase, 30 cycles, 72 °C annealing, 30 sec elongation) to introduce indexed Illumina-TruSeq-like adapters (primer Ill-ONP-P7-bi7NN and Ill-ONP-P5-bi5NN). The products were size selected on a 3% NuSieve 3:1 Agarose gel (Lonza), purified using NucleoSpin Gel and PCR clean-up columns, and quantified on a Qubit Fluorometer (dsDNA HS Assay Kit, Thermo Fisher Scientific) and by qPCR (NEBNext Library Quant, New England Biolabs, LightCycler480, Roche). SIC pools were processed likewise using tRNA-seqNN and mNeon-seqNN as primers to introduce UMIs. All samples were pooled according to the designed complexity and sequenced on a NextSeq 550 system (Illumina) with 300 cycle paired-end chemistry.

Estimation of recombineering fidelity in libraries shown in Fig. 4.: We sequenced the oligonucleotide pool after PCR amplification, and the SIC pool obtained from the recombineering procedure. In the latter instance, fragments compatible with Illumina NGS were generated by breaking down the products of rolling circle amplification with *Bts*$^{\alpha}$I (55 °C, 90 min, New England Biolabs) and *Sal*I-HF (37 °C, 90 min, New England Biolabs). The fragments were column-purified, diluted to 100 ng/µL and blunted using 1 U/µg mung bean nuclease under the appropriate buffer conditions (New England Biolabs). The DNA fragments of 150–200 bp length were gel-extracted on 3% NuSieve 3:1 Agarose (Lonza). Both samples were sequenced by GATC Biotech AG (Konstanz, Germany) using Illumina MiSeq 150 paired-end NGS technology.

T**ransformation of SICs.** For transformation of individual 'self-integrating' cassettes (SICs) or SIC pools, Cas12a (Cpf1)-family proteins were transiently expressed by making (1) frozen competent cells using either yeasts strains with *GAL1*-controlled Cas12a (Cpf1) proteins grown in YP or SC medium containing 2% (w/v) raffinose and 2% (w/v) galactose as carbon source or (2) yeast strains with *TEF1*-promoted Cas12a (Cpf1) expression grown in SC –Ura to select for the presence of the plasmid. For transformation[5], the heat shock was extended to 40 min and no DMSO was added. Recovery of cells that required selection for dominant antibiotic resistance markers (G-418, hygromycin B and clonNAT[6]) was allowed for 5–6 hours at room temperature in YP-Raf/Gal or YPD to proceed prior to plating them on corresponding selection plates.

SIC pools were transformed at a total of 1 µg per 100 µL of frozen competent yeast cells. Per library approximately 5 of such transformation reactions were combined corresponding to a yeast culture volume of 50 to 100 mL (OD_{600} = 1.0) to generate the competent cells. The number of transformants per library was calculated from serial dilutions. Replica-plating on selective plates was used to exclude transiently transformed clones. After outgrowth, libraries were harvested in 15% glycerol and stored at –80 °C. For subsequent experiments including genotyping, approximately 10,000 cells per clone were inoculated in YPD, diluted to OD_{600} = 1.0 (approx. 50 mL of culture), and grown over-night. If necessary, a second dilution was performed to obtain cells in exponential growth phase.

For co-integration experiments using individual SICs, 1 µg DNA per SIC and condition was transformed using 50 µL competent yeast cells. Colony number and fluorescence images were acquired after the sample had been spread onto selective plates. Potential co-integrands were tested by replica-plating, streaking and fluorescence microscopy.

Each transformation mixture was split into two parts containing 1/20 (libA) or 19/20 (libB) of the volume. The largest sample was plated onto four 25 x 25 cm square plates with YPD + G-418. No replica-plating was performed before the libraries were cryo-preserved in 2.5 mL, 10 mL, and 50 mL 15% glycerol respectively.

For libraries libC, and the small nuclear library (based on P1), the transformation mixture was plated onto two 25 x 25 cm plates with YPD + hygromcycin B.

Fluorescence microscopy. Cells were inoculated at an OD_{600} = 0.5 per condition in 5 mL low-fluorescent SC medium (SC-LoFlo[7]) from cryopreservation stocks and grown over night, followed by dilution to OD_{600} = 0.1 in 20 mL SC-LoFlo the next morning and imaging during exponential growth in the afternoon. High-resolution fluorescence micrographs were taken on a Nikon Ti-E epifluorescence microscope equipped with a 60 x ApoTIRF oil-immersed

objective (1.49 NA, Nikon), a 2048 x 2048 pixel (6.5 µm), an sCMOS camera (Flash4, Hamamatsu) and an autofocus system (Perfect Focus System, Nikon) with either bright field, 469/35 excitation and 525/50 emission filters or 542/27 excitation and 600/52 emission filters (all from Semrock except 525/50, which was from Chroma). For each condition, a z-stack of 10 planes at 0.5 µm distance was acquired each with a bright field, a short (75% excitation intensity, 10 ms) and a long fluorescence exposure (100% excitation intensity, 100 ms) regimen. For display, the fluorescent image stacks were z-projected for maximum intensity, and cell boundaries taken from out-of-focus bright field images.

Fluorescence-activated cell sorting (FACS). A homogenous population of small cells (mostly in G1 phase of the cell cycle) was selected using forward and side scatter. Single cells were sorted according to fluorescence intensity using a FACS Aria III (BD Diagnostics) equipped for the detection of green (excitation: 488 nm, long pass: 502LP, band pass: 530/30) or red fluorescent proteins (excitation: 561 nm, long pass: 600LP, band pass: 610/20). We first isolated fluorescent cells (3 million in total), which represented roughly 30% of the cells in library #1.1 (Supplementary Table 2) as judged against cells from strain ESM356-1 as a negative control. The population of fluorescent cells was then grown to exponential phase and sorted into eight fractions of 125,000 cells each using bin sizes of roughly 5% (bin 1), 20%, 20%, 20%, 25%, 5%, 5%, 1% (bin 8) according to the intensity of fluorescence emission of small (G1) cells. Sorted pools were grown over-night and the cells were harvested for genomic DNA extraction and target enrichment NGS.

Library characterization by Anchor-Seq. To determine cassette integration sites in CASTLING libraries, we used a modified Anchor-Seq protocol[8]: Libraries depicted in Fig. 4 were prepared with vectorette bubble adapters (vect_illumina-P5 and vect_illumina-P7) that themselves contained barcodes for multiplexing several samples in the same sequencing run. For all other libraries (Fig. 3 and Fig. 5), the adapters contained UMIs to account for PCR bias during NGS library preparation; the barcodes for multiplexing were introduced at the stage of the Illumina sequencing adapters. Genomic DNA (gDNA) was isolated from a saturated overnight culture (approximately 2 x 10^8 cells) using YeaStar Genomic DNA Kit (Zymo Research). Genomic DNA (125 µL at 15 ng\µL in ultrapure water) was fragmented by sonication to 800–1,000 bp in a microTUBE Snap-Cap AFA Fiber on a Covaris M220 focused ultrasonicator (Covaris Ltd.). In our hands, 51 sec shearing time per tube, a peak incident power of 50 W, a duty factor of 7% and 200 cycles per burst robustly yielded the required size range. Adapters were prepared by combining 50 µM of the respective Watson- and Crick-oligonucleotides (Supplementary Table 9). Each mixture was heated up to 95 °C for 5 min followed by cooling to 23 °C in a large water bath over the course of at least 30 min. Annealed adapters were stored at –20 °C until use. We prepared an equimolar

mixture of annealed adapters that contained either none, one, or two additional bases inserted after the UMI (halfY-Rd2-Watson and halfY-Rd2-NN-Crick) to increase heterogeneity of the sequencing library. The fragmented genomic DNA (55.5 µL) were end-repaired and dA-tailed (NEBNext Ultra End Repair/dA-Tailing Module, New England Biolabs) and ligated to 1.5 µL of the 25 µM annealed adapter mix (NEBNext Ultra Ligation Module, New England Biolabs). Products larger than 400 bp were purified by gel excision (using NuSieve, described above) and eluted in 50 µL 5 mM Tris-HCl (pH = 8.5). SIC integration sites were enriched by PCR (NEBNext Ultra Q5 Master Mix, New England Biolabs) using 12 µL of the eluate with suitable pairs of adapter- and SIC-specific primers. Initial denaturation was 98 °C (30 sec), followed by 15 cycles of 98 °C (10 sec), and 68 °C (75 sec). Final extension was carried out at 65 °C (5 min). Reactions were cleaned-up using Agencourt AMPure XP beads (0.9 vol, Beckman Coulter). The fragments were further enriched in a second PCR using the custom-designed primers Ill-ONP-P7-bi7NN and Ill-ONP-P5-bi5NN to introduce technical sequences necessary for multiplexed Illumina sequencing. After size-selection by gel extraction (250–600 bp), NGS library concentrations were measured by Qubit Fluorometer (dsDNA HS Assay Kit, Thermo Fisher Scientific) and by qPCR (NEBNext Library Quant, New England Biolabs, LightCycler480, Roche). Furthermore, their size distribution was verified either on a Fragment Analyzer (Advanced Analytical Technologies, Inc) or by gel electrophoresis of the qPCR product. Quantified libraries were sequenced on a NextSeq 500 (for P2, Deep Sequencing Core Facility) or on a NextSeq 550 sequencing system (both Illumina, 300 cycle paired-end). If necessary, 10–15% phiX gDNA was spiked in to increase sequence complexity.

For Oxford Nanopore Technologies NGS, just the first PCR of P2 was carried out as described above (using 20 cycles), column-purified, and the NGS library was prepared for 1D sequencing by ligation (SQK-LSK108) according to the manufacturer's protocols (Oxford Nanopore Technologies). Sequencing was performed on a MinION device using R9.4 chemistry. Samples from multiple libraries or bins after FACS were multiplexed considering the number of different clones present in a pool, bin size, gDNA yield after extraction, and yield of the first PCR.

Processing of high-throughput sequencing results and read counting. *For Illumina NGS*: Raw reads (150 bp paired-end) were trimmed and de-multiplexed using a custom script written in Julia v0.6.0 with BioSequences v0.8.0 (https://github.com/BioJulia/BioSequences.jl). Read pairs were retained upon detection of basic Anchor-Seq adapter features. Next, these reads were aligned to a reference with all targeted loci using bowtie2[9] v2.3.3.1. Such references comprised the constant sequence starting from the feature cassette amplified by PCR and 600 bp of the respective proximal genomic sequence of

Saccharomyces cerevisiae strain S288C (R64-2-1). For off-target analysis the constant Anchor-Seq adapter features were trimmed off the reads. The remaining variable sequence of the reads were then aligned with bowtie2 to the complete and unmodified genome sequence of *Saccharomyces cerevisiae* strain S288C (R64-2-1). A read pair that aligned to the reference was counted if both reads of the pair were aligned, such that the forward read started at the constant region of the Anchor-Seq adapter-specific primers. In addition, we set the requirement that the inferred insert size was longer than the sequence material provided for homologous recombination during the tagging reaction. Counting was implemented using a custom script (Python v3.6.3 with HTSeq 0.9.1 and pysam 0.13). In case UMIs were included in the Anchor-Seq adapter design (libraries created from pools P2 or P3), they were normalized for sequencing errors using UMI-tools[10].

For analysis of data obtained from amplicon sequencing (i.e. from PCR and SIC amplification reactions), the reads were either denoised from sequencing errors to evaluate fidelity and abundance or directly aligned with bowtie2 to a reference build from the designed oligonucleotides. Denoising was based on minimal hamming distance to designed oligonucleotides using dada2 (version 1.5.2[11]).

For Oxford Nanopore NGS: Nanopore sequencing yields very long reads, therefore the reference was assembled as aforementioned but using 2,000 bp of the locus-specific sequences. For data analysis, a custom script was used to extract and de-multiplex informative sequence segments from all reads using base calls obtained from the Albacore Sequencing Pipeline Software v2.0.2 (ONT) based on approximate matching of amplicon features (e.g. the constant region of the vectorette or feature cassette) with a Levenshtein distance of maximal 20% (Julia v0.6.0 with BioSequences v0.8.0, see above). This was sufficient to discriminate between the barcodes used in this study. Then, the extracted sequence segments were aligned to the reference using minimap2 (v2.2-r409, https://arxiv.org/abs/1708.01492) using the default parameters (command line option: '-ax map-ont') for mapping of long noisy genomic reads. Only reads that mapped to the beginning of the reference were counted using a custom shell script. The count data for the clones retrieved in each library for the fluorescent cell enriched population and for cells contained in the individual bins after FACS are provided in Supplementary Table 3. Genotypes were scored by presence or absence in the individual FACS fractions.

Calculations and statistical analyses. Statistical analyses were performed using *R* as specified in the scripts or legends.

Estimation of co-integrand number. We assumed that most co-integrands would result from doubly transformed individuals. So, the number of phenotypic 'heterozygous' individuals (e.g. GFP+ RFP+ or kan^R hyg^R) represents half of the co-integrands if both feature cassettes

that were transformed at equimolar ratios have equal probability to be taken up with the likes of them (i.e. GFP+ GFP+ and RFP+ RFP+) as with each other. Further, we assumed that the fluorescent protein or the antibiotic resistance marker present in the feature cassette had no or only a minor impact on integration efficiency.

Software and figure generation. Proportional Venn diagrams were generated using eulerAPE[12]. Analyses were performed using R v3.4.1/v3.5.1 with Biostrings v2.44.2[13] and data.table v1.10.4/v1.11.4. Plots were generated using ggplot2 v2.3.0 and figures were made using Apple Keynote 8.2.

Computer code availability. The source code of the R shiny application for oligonucleotide design is available from our github repository (https://github.com/knoplab/castR).

References for Online Methods.

1. Brachat, A., Kilmartin, J. V., Wach, A. & Philippsen, P. Saccharomyces cerevisiae cells with defective spindle pole body outer plaques accomplish nuclear migration via half-bridge-organized microtubules. *Mol Biol Cell* **9,** 977–991 (1998).
2. Winston, F., Dollard, C. & Ricupero-Hovasse, S. L. Construction of a set of convenient Saccharomyces cerevisiae strains that are isogenic to S288C. *Yeast* **11,** 53–55 (1995).
3. Zetsche, B. *et al.* Cpf1 is a single RNA-guided endonuclease of a class 2 CRISPR-Cas system. *Cell* **163,** 759–771 (2015).
4. Johnston, M. A model fungal gene regulatory mechanism: the *GAL* genes of *Saccharomyces cerevisiae*. *Microbiol. Rev.* **51,** 458–476 (1987).
5. Knop, M. *et al.* Epitope tagging of yeast genes using a PCR-based strategy: more tags and improved practical routines. *Yeast* **15,** 963–972 (1999).
6. Janke, C. *et al.* A versatile toolbox for PCR-based tagging of yeast genes: new fluorescent proteins, more markers and promoter substitution cassettes. *Yeast* **21,** 947–962 (2004).
7. Sheff, M. A. & Thorn, K. S. Optimized cassettes for fluorescent protein tagging in Saccharomyces cerevisiae. *Yeast* **21,** 661–670 (2004).
8. Meurer, M. *et al.* Genome-wide C-SWAT library for high-throughput yeast genome tagging. *Nature Methods* **15,** 598–600 (2018).
9. Langmead, B. & Salzberg, S. L. Fast gapped-read alignment with Bowtie 2. *Nature Methods* **9,** 357–359 (2012).
10. Smith, J. D. *et al.* A method for high-throughput production of sequence-verified DNA libraries and strain collections. *Mol. Syst. Biol.* **13,** 913 (2017).
11. Callahan, B. J. *et al.* DADA2: High-resolution sample inference from Illumina amplicon data. *Nature Methods* **13,** 581–583 (2016).

12. Micallef, L. & Rodgers, P. eulerAPE: Drawing Area-Proportional 3-Venn Diagrams Using Ellipses. *PLoS ONE* **9,** e101717 (2014).

13. Pagès, H., Aboyoun, P., Gentleman, R. & DebRoy, S. *Biostrings: String objects representing biological sequences, and matching algorithms. R package version 2.40.2*. (2016).

SUPPLEMENTARY INFORMATION FOR

Pooled clone collections by multiplexed CRISPR/Cas12a-assisted gene tagging in yeast

Benjamin C. Buchmuller, Konrad Herbst, Matthias Meurer, Daniel Kirrmaier, Ehud Sass, Emmanuel D. Levy, Michael Knop

CONTENTS

SUPPLEMENTARY NOTES

1. Design of an oligonucleotide pool for C-terminal tagging of yeast ORFs

The design principles described below are implemented in R (Script 1). For oligo design the annotated yeast reference genome was retrieved from the *Saccharomyces* Genome Database[1] (www.yeastgenome.org, November 2016), which contained 5,743 chromosomal yeast ORFs. This process consists of three stages. In stage 1 the CRISPR target sequences are retrieved and evaluated; in stage 2 the corresponding oligonucleotides are constructed *in silico* and evaluated; and in stage 3 the selection of oligonucleotides is further confined to optimally use pool synthesis capacity.

Stage 1. For C-terminal tagging, all protospacer-adjacent motifs (PAMs) of the selected CRISPR/Cas12a endonuclease within ±30 nt around the STOP codon were retrieved. For tagging with FnCpf1, these PAMs were TTV and TYN in the first genome-wide pool design and TTV in the second genome-wide pool design. If a PAM was followed by another PAM, only the downstream PAM was considered to obtain non-adjacent CRISPR target sequences ('spacers') only. In the next step, the 20 nt long target sequences were extracted. Target sequences that contained runs of more than five thymidine bases were removed to avoid pre-mature termination of crRNA transcription by RNA polymerase III. Spacers pre-maturely abrogating transcription by ending with T or TT were not removed because 18 nt spacers can still be functional[2].

For the remaining spacers, we established (1) whether the genomic target sequence would be removed by SIC integration, i.e. whether it spanned the STOP codon, and (2) the risk of off-target cleavage. This risk was assessed as the number of genome-wide occurrences of these sequences (including PAM-free sites) permitting mismatches in the spacer according to the following rules: maximum 1 base mismatch in the crRNA seed, i.e. the first eight PAM-proximal nucleotides, and/or maximum 3 mismatched bases in the entire target sequence. In total, 37,438 TTV sites and 45,445 TYN sites were evaluated during the first genome-wide pool design.

Stage 2. Oligonucleotides are constructed as outlined in Supplementary Fig. 6. In brief, the length of each homology arm is established first. Any bases potentially removed from the open reading frame (ORF) or the 3' untranslated region (3' UTR) after target cleavage by the CRISPR endonuclease are reconstituted by the homology arms after SIC integration.

Next, the oligonucleotides are assembled starting with the last ~30 nt of the crRNA expression unit, i.e. of the *SNR52* promoter (first genome-wide pool design) or the tG(GC)F2 tRNA site (second genome-wide pool design). In both designs, the next element is the direct repeat sequence of FnCpf1 and the target-specific spacer sequence determined in stage 1. Following, the 3' homology arm, a restriction site used in the recombineering procedure (*Bst*XI in both designs), the 5' homology arm (without the STOP codon) and finally an in-frame linker, such as a Thr-Ser linker or a S1/S3 linker. The linker serves as generic recombineering site with the feature cassette encoding the desired reporter gene.

After *in silico* design, oligonucleotide sequences that contain more than one of the endonuclease restriction sites are removed. Therefore, it is advised to choose a restriction enzyme with low restriction site frequency at the desired tagging site. For C-terminal tagging in yeast, we considered *Bst*XI or *Ngo*MIV in the first pool design (16,005 remaining TTV candidates; 18,720 remaining TYN candidates) and *Bst*XI in the second pool design (32,602 remaining TTV candidates).

Stage 3. Since the number of candidate oligonucleotide designs typically exceeds the synthesis capacity for a single array-based oligonucleotide pool, a selection procedure for pool assembly is required.

In the first genome-wide pool design, this was effected as follows: All ORFs that were targeted by a single oligonucleotide only were preserved regardless of the following criteria. For all other ORFs, oligonucleotides that contained a spacer with low off-target estimate and/or the ability to remove the genomic target by SIC integration were preferred. The final pool contained 12,472 oligonucleotide sequences for tagging 5,664 ORFs.

In the second genome-wide pool design, we tried to consider the parameters previously identified to improve tagging success. Therefore, oligonucleotide candidates were ranked based on a bonus-system. For each ORF, the three oligonucleotides with the highest bonus were selected (17,691 oligonucleotides). We also included designs that had proven repeatedly successful in the first genome-wide pool design, summing up to 18,752 sequences. Another 8,248 candidate oligonucleotides were included by random draw to use up the remaining synthesis capacity of this pool (27,000 oligonucleotides) for tagging 5,940 ORFs.

CASTLING and gene drive

1.1. Circumstances under which CASTLING can generate a gene drive-system

The co-occurrence of a gene with a molecular machinery that is suited to propagate itself along with that gene from one chromosome to a homologous one, leading to homozygotization of the gene locus with the propagation machinery biases the inheritance of this gene within sexually reproducing populations towards much higher transmission frequencies than expected from sexual inheritance ('gene drive'). Importantly, the strength of the gene drive depends primarily on the fidelity and efficiency by which the element is copied, and less on the nature of the gene that is driven. In each generation, genes that decrease the fitness of an individual can spread just as efficiently as genes that confer e.g. resistance to antibiotics, leading to potentially harmful or undesired effects on the host population ('population replacement'[3,4], spread of resistances[5]).

Artificial genetic elements that combine the expression of an RNA-programmable endonuclease (i.e. Cas9 or Cas12a) and a gene from which a cognate crRNA is expressed can exhibit gene drive in a process reminiscent of gene conversion[6].

CASTLING bears the risk of accidentally crating such an artificial drive system if one of the 'self-integrating' cassettes is targeted to the neighborhood of a stably integrated, actively expressed Cas12a-endocing gene (Supplementary Figure 10). In such a constellation, the crRNA expressed from the gene engineered by CASTLING could cleave the homologous chromosome and thereby induce repair of the damaged locus with the information of the engineered chromosome. If the CRISPR endonuclease-encoding locus is copied along with the repair template during this process, homozygotization of the drive system is complete. Thus, the likeliness and the strength of the drive depends on the distance between the Cas12a and the crRNA gene, i.e. on the amount of sequence between them that is homologous to the sequence on the homologous chromosome. The exact distance that will eliminate gene drive capabilities is not known, but given the fact that already 36 bp in *S.*

cerevisiae (which may be different for other hosts) are sufficient to promote homologous recombination efficiently, we expect that the ability to 'drive' will be lost or strongly reduced if the Cas12a gene and the crRNA gene are separated by more than a few hundred base pairs of sequence that is homologous to the other chromosome.

1.2. Safety and security measures

Based on these considerations we strongly recommend the following safety measures that are effective to prevent the accidental creation of an artificial genetic element that exhibits gene drive using CASTLING in sexually reproducing organisms:

- The Cas12a (Cpf1) endonuclease can be contained on an episomal plasmid that is not prone to integrate into the genome. Plasmids that contain counter-selectable markers such as *URA3* can be used to enforce the loss of the Cas12a after library preparation.
- In case a strain with a genomically integrated Cas12a gene is used, the SICs should not target sequences in proximity to the Cas12a locus. In this situation, occasional spontaneous integration of the plasmids into the genome must be considered and care must be taken that none of the SICs can target the plasmid itself. Creating such crRNAs can be avoided by removing (or masking) all sequences that fulfill these criteria from the host reference genome sequence before starting with oligonucleotide pool design.

If these minimal requirements are met and if all the generated genetically modified organisms (GMOs) are contained properly during the experiment, we believe that CASTLING bears no risk of gene drive creation.

SUPPLEMENTARY FIGURES

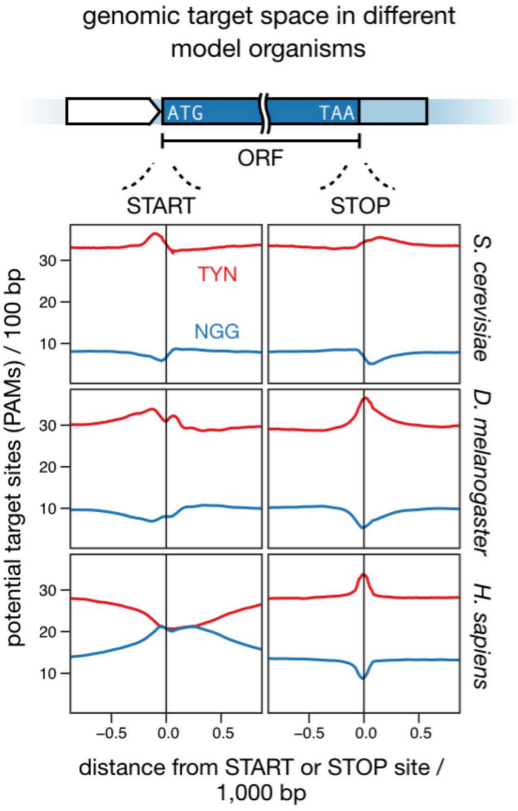

Supplementary Figure 1. Genomic target space in different organisms considering PAM sites from Cas9 and Cas12a endonucleases.

The frequency of the protospacer-adjacent motifs (PAMs) for CRISPR/Cas9 (NGG) and CRISPR/Cas12a (TYN) endonucleases per 100 bp (sliding-window, increment 10 bp) ±1 kb around the START (ATG) and STOP codon (e.g. TAA) of open-reading frames (ORFs) in different organisms is shown. As previously reported[7], GC-content usually drops or peaks at such sites.

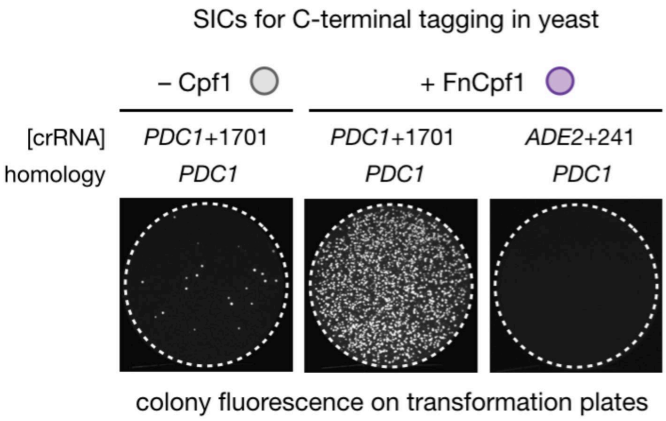

Supplementary Figure 2. Specific and efficient SIC integration in CASTLING.

Transformation of a SIC for C-terminal tagging of *PDC1* using 50 nt homology arms, with and without expression of Cas12a of *Francisella novicida U112* (FnCpf1), or with a crRNA targeting *PDC1* at base +1701, or the *ADE2* locus at base +241 (*ade2* knock-out observed).

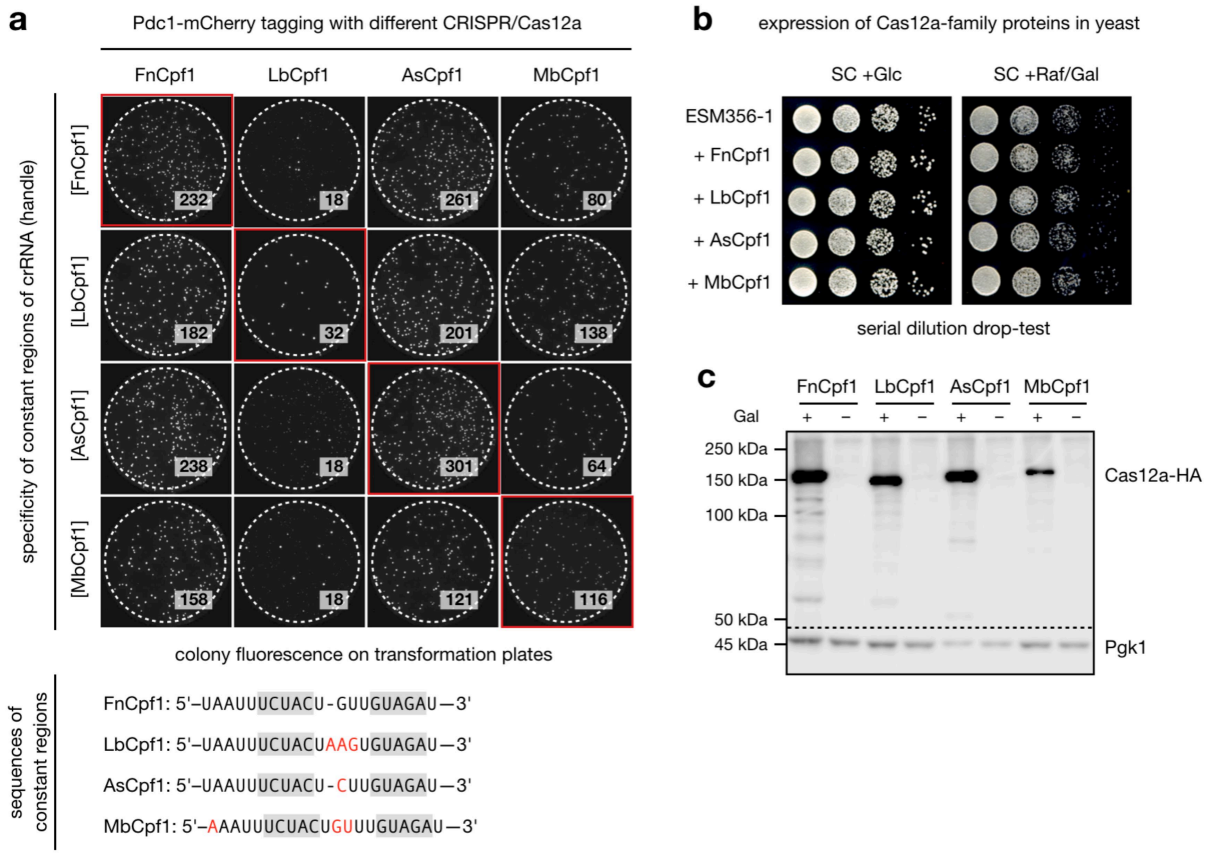

Supplementary Figure 3. Evaluation of Cas12a-family proteins and expression systems for gene tagging using 'self-integrating cassettes' in yeast.

(**a**) Combinatorial testing of four different CRISPR/Cas12a-family proteins and four different constant regions ('handles') of the crRNA for tagging *PDC1* with a red fluorescent reporter protein (mCherry) by means of [crRNA]*PDC1*+1701 (same PAM, TTTA, in all cases). Colony fluorescence is shown after spread-plating the transformation reaction and outgrowth; numbers indicate the fluorescent colonies growing on the plates after replica-plating. The results demonstrate that integration efficiency of SICs is less dependent on the handle than on the identity of the Cas12a protein.

(**b**) Serial dilutions of yeast cultures to test potential toxicity of different CRISPR/Cas12a-family proteins[2] under expression from a glucose-repressed/galactose-inducible promoter, namely Cas12a of *Francisella novicida U112* (FnCpf1), *Lachnospiriceae bacterium ND2006* (LbCpf1), *Acidaminococcus sp. BV3L6* (AsCpf1), and *Moraxella bovoculi 237* (MbCpf1). None of these Cas12a exhibited toxicity in yeast under these conditions.

(**c**) Expression of all tested Cas12a variants was confirmed by immunoblotting (lower panel). Yeast cell extract was normalized to total cell number 3.5 h post induction with 2% galactose. When grown in 2% raffinose as sole carbon-source (–), Cas12a protein levels were below the limit of detection. The Cas12a-family proteins were detected using a

hemagglutinin tag and stained by monoclonal antibodies (12CA5, Sigma-Aldrich). Pgk1 (44.7 kDa) was stained as loading control and detected using monoclonal mouse anti-Pgk1 antibodies (R & D Systems, Fisher Scientific).

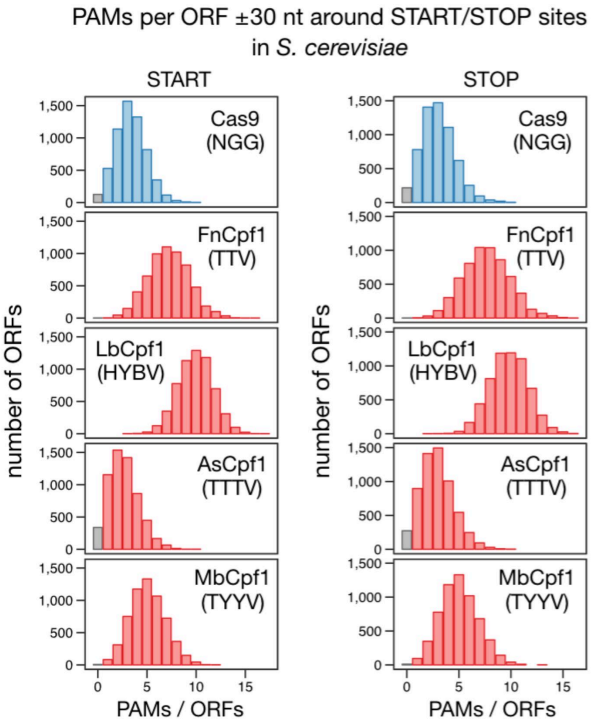

Supplementary Figure 4. Genomic target space of different CRISPR/Cas12a proteins in yeast.

Using CRISPR-Cas12a family proteins, many open-reading frames (ORFs) in yeast can be targeted at multiple sites near (±30 nt) the START or STOP codon. The target space ranges from 83% (AsCpf1) to 99% (FnCpf1) considering all annotated ORFs (retrieved from the *Saccharomyces* Genome Database[1], www.yeastgenome.org, November 2016).

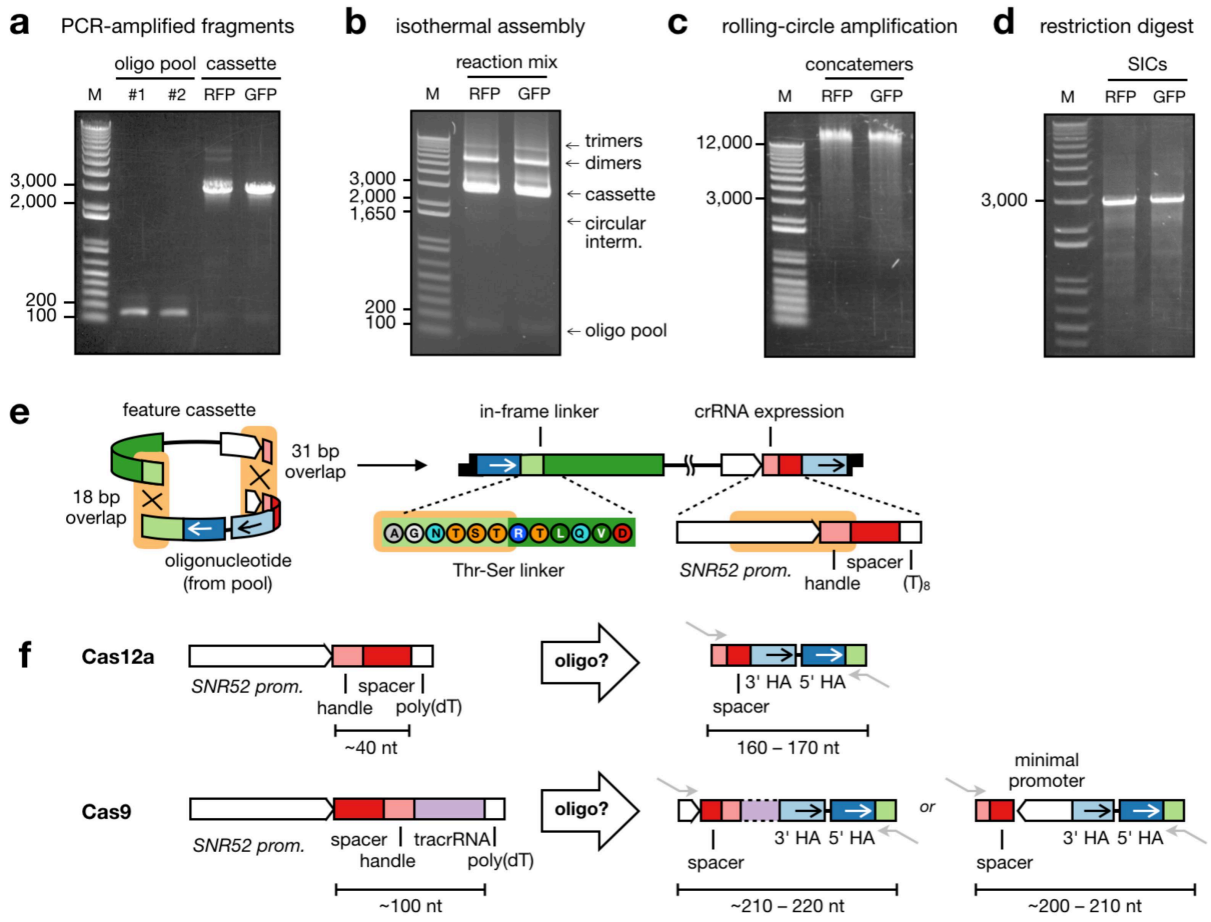

Supplementary Figure 5. Molecular *in vitro* recombineering procedure to create 'self-integrating' cassettes (SICs) from a pool of oligonucleotides. *a–d* displaying agarose gel electrophoresis images of the starting materials, different intermediates and the final SICs.

(**a**) The oligonucleotide pool (< 170 bp) and the desired feature cassettes (here: 2–3 kb, but can be shorter or longer) are PCR-amplified (to introduce short homologous overhangs (15–30 bp) for isothermal assembly).

(**b**) Molecular recombineering by isothermal assembly yields the 'self-integrating cassettes' (SICs) as a covalently-closed circular DNA along with reaction by-products. The circular DNA constitute a minor fraction of the reaction product and for further processing the smallest band is isolated (circular intermediates).

(**c**) The circular DNA serves as a template for random-primed isothermal rolling-circle amplification (RCA) to generate very long (>12 kb) linear dsDNA by means of a highly processive DNA-polymerase with strong strand-displacement capabilities such as phi29 DNA-polymerase. Each linear dsDNA is a concatemer repeating a single SIC.

(**d**) Restriction digestion with a suitable restriction enzyme (here: *Bst*XI) breaks down the long dsDNA molecules into SIC monomers through cleavage of the sequence that linked the homology arms in the designed oligonucleotides.

(**e**) Specification of overlap length for isothermal assembly that collapse into an in-frame peptide linker and a functional gene to drive crRNA expression.

(**f**) Minimal requirements to provide all locus-specific elements on a single oligonucleotide. For Cas12a (Cpf1), the constant crRNA handle (20 nt) can be part of the primer binding site, and thus the total length of the oligo ranges 160–170 nt. For Cas9, additional elements must be provided inside the oligo, either a tracrRNA (60 nt) that can be fused with the crRNA to yield a sgRNA (90 nt) or – to reverse the orientation of the elements – a minimal constitutive RNA-polymerase III promoter (35 nt). In total, such oligonucleotides would range 200–220 nt in length. Given current limitations in oligonucleotide synthesis, shorter oligonucleotides (i.e. the Cas12a design) are preferred.

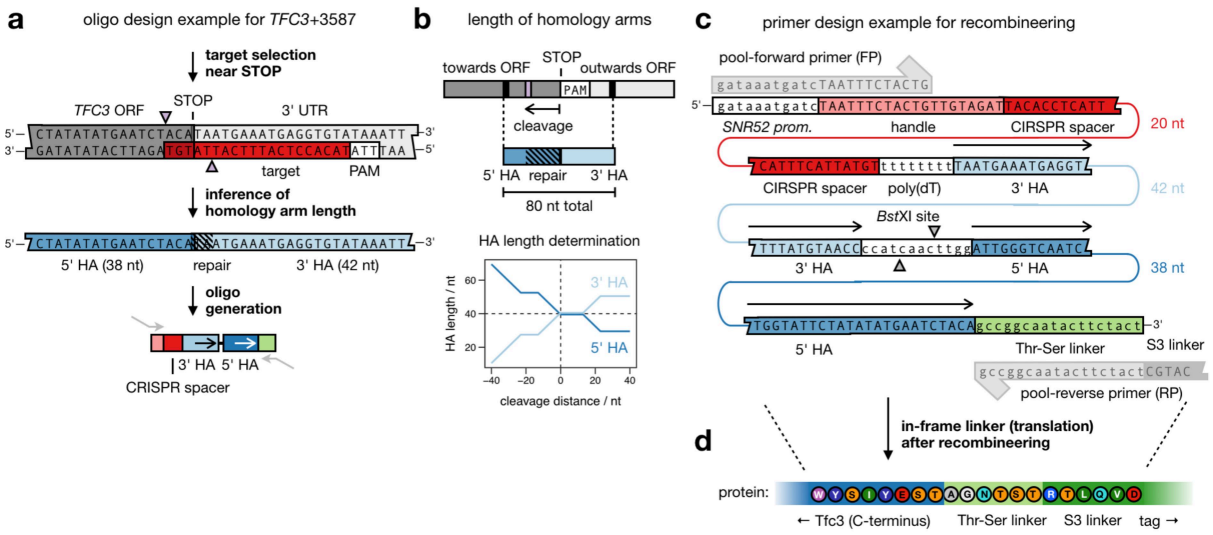

Supplementary Figure 6. Design example for an oligonucleotide to create a SIC for tagging the gene *TFC3* at position +3587, near the STOP codon.

(**a**) Locus-specific elements that are included in the oligonucleotide are the CRISPR spacer complementary to the target sequence for CRISPR/Cas12a, and the homology arms that precisely end and start with the STOP codon for C-terminal tagging.

(**b**) The length of homology arms is chosen to always sum up to a total of 80 nt (for space constraints on the oligonucleotide). If the DNA double-strand break occurs upstream of the STOP codon, a part of the 5' homology arm (HA) serves to reconstitute the lost sequence information and is therefore chosen longer. Experimentally, we determined that homology arms as short as 20 nt still function efficiently to guide correct insertion of the SICs (data not shown).

(**c**) Primer design example (as used for the libraries in Fig. 4, ID #1.1–1.3 in Supplementary Table 2) for the forward (FP) and reverse primer (RP) of pool amplification. The FP overlaps with the *SNR52* promoter that drives crRNA expression, the RP translates in an in-frame linker between the ORF and the desired tag.

(**d**) In-frame linker after C-terminal tagging of Tfc3.

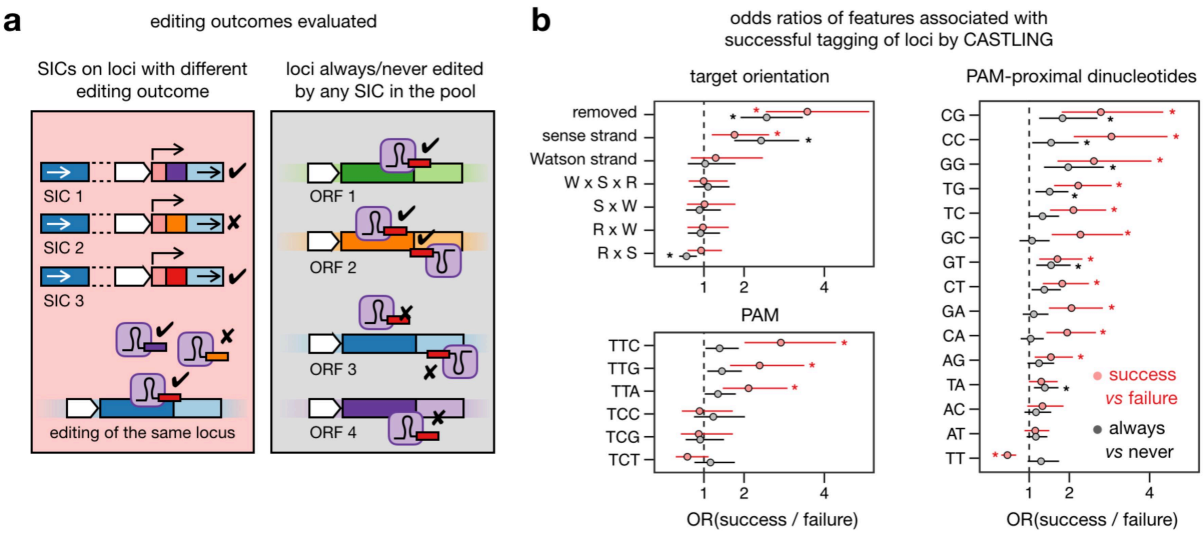

Supplementary Figure 7. Features of the crRNA and target locus associated with successful tagging.

(**a**) Details to the analysis shown in Fig. 4. Two scenarios were considered as represented by red and grey panels. Scenario 1 (red panel) considers all SICs demonstrably present in the SIC pool for the same gene to be tagged, comparing them based on the editing outcome (success: *N* = 2,053 SICs; failure: *N* = 2,488 SICs). Only genes were included in this analysis, that had both, successful and non-successful SICs. Scenario 2 (gray panel) compares tagging success for genes, in which any of the designed SICs promoted (total *N* = 2,885 SICs) or failed (*N* = 3,209 SICs) to tag the gene.

(**b**) Odds ratio (OR) based on samples drawn akin to (*a*) based on multiple logistic regression analysis. Asterisks indicate properties for which the impact on odds is significantly ($p < 0.01$) different from 1 (no effect); error bars represent 95% confidence intervals). All scenarios displayed were checked for inter-dependencies (indicated as 'A x B') also in-between the panels with no effect on the general outcome, but were split for the sake of clarity. 'Sense strand' refers to the genomic target occurring on the non-transcribed strand, whereas 'Watson strand' is any of the two strands as specified in the yeast gene nomenclature. 'Nucleosome occupancy at the PAM' or across the entire 'target sequence'[8] and 'gene expression in YP-Raf/Gal' (medium to transiently express FnCpf1) or 'YPD'[9] (to suppress FnCpf1 expression) were also analyzed with no significant impact on tagging success (data not shown).

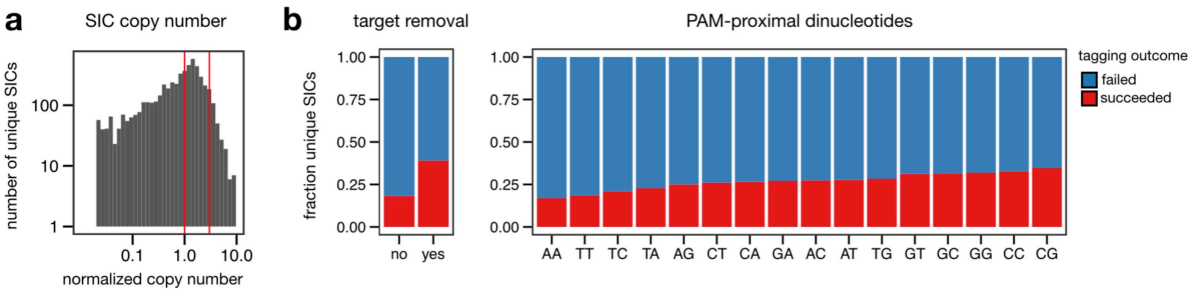

Supplementary Figure 8. Verification of features of the crRNA and target locus associated with successful tagging.

(**a**) As copy number after RCA has a major impact on tagging success upon transformation, a set of SICs with approximately equal copy number (1- to 3-fold of the median copy number) was analyzed.

(**b**) Comparison of tagging success (color code) for SICs grouped according to their removing the genomic target site by integration (left panel) and first PAM-proximal dinucleotides in the crRNA sequence (right panel). In both cases, tagging success was higher when the rule set (Supplementary Fig. 7) was obeyed.

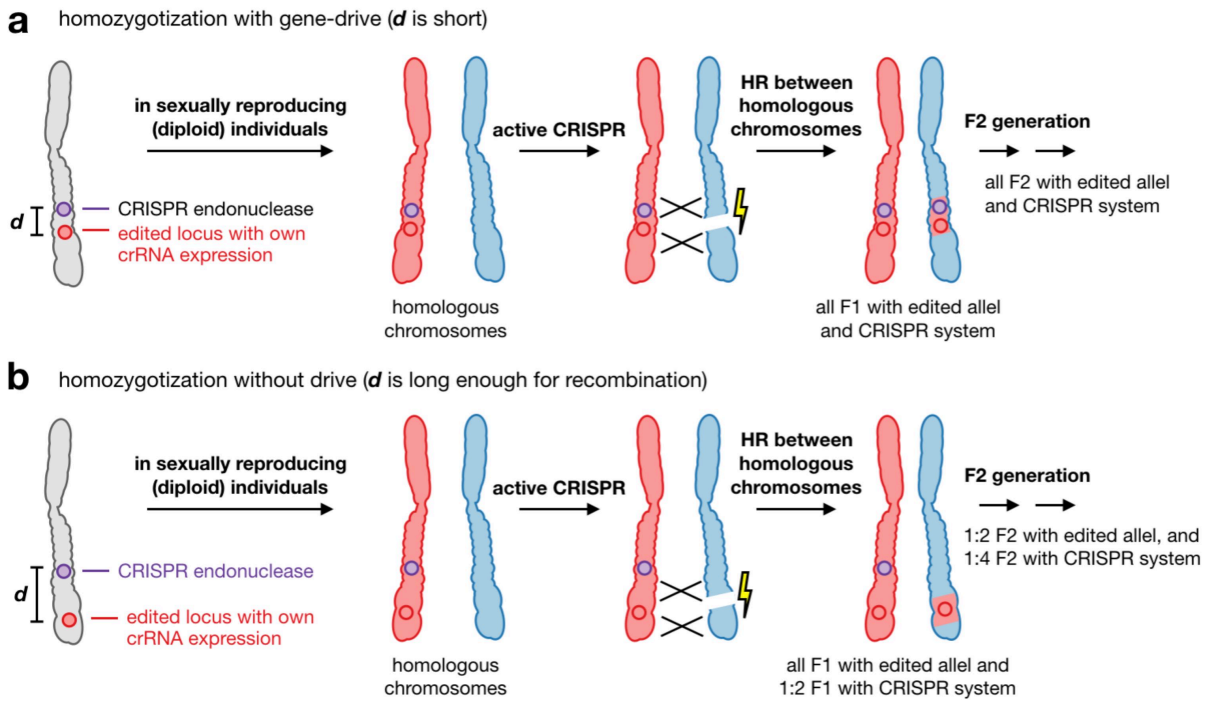

Supplementary Figure 9. Mechanism of allele homozygotization and potential 'gene drive' with stably integrated CRISPR endonucleases (Supplementary Notes).

(**a**) If the distance (***d***) of the crRNA expression site and the endonuclease locus is very short, homozygotization of both loci is highly likely (gene drive).

(**b**) With increasing ***d***, the likelihood that both genes are copied to the homologous chromosome decreases.

SUPPLEMENTARY TABLES

Supplementary Table 1. Library statistics for libraries created from pools P1A–C (Fig. 3).

ID	oligo pool	PCR pool (after amplification)			feature cassette	SIC pool (after recombineering/RCA)			clone collections (libraries)			
		primer	reads mapped	identified unique sequences, ORFs (UMI >2)		pooled RCA reactions	reads mapped	identified unique sequences, ORFs (UMI > 2)	clones	library stock	reads mapped	identified unique sequences, ORFs (UMI >2)
1a	P1A, 40.0 ng (0.8 pmol)	pool-FP3 + pool-RP3	152,011	1,200 seq. (76%), 206 ORFs (96%)	pKH51	2	125,015	493 seq. (31%), 147 ORFs (68%)	58,000	YKH231	277,026	280 seq. (18%), 125 ORFs (58%)
1b			195,535	1,281 seq. (81%), 209 ORFs (97%)	pKH51	2	70,984	324 seq. (20%), 116 ORFs (54%)	64,000	YKH232	266,519	202 seq. (13%), 107 ORFs (50%)
2a	P1B, 150. pg (3.0 fmol)	pool-FP2 + pool-RP2	265,556	1,308 seq. (83%), 209 ORFs (97%)	pKH51	3	177,648	872 seq. (55%), 191 ORFs (89%)	82,000	YKH227	443,204	496 seq. (31%), 172 ORFs (80%)
2b			253,732	1,333 seq. (84%), 209 ORFs (97%)	pKH51	2	225,114	601 seq. (38%), 179 ORFs (83%)	81,500	YKH228	478,846	309 seq. (19%), 144 ORFs (67%)
3a	P1C, 150. pg (3.0 fmol)	pool-FP3 + pool-RP3	148,529	1,454 seq. (92%), 211 ORFs (98%)	pKH51	2	44,005	825 seq. (52%), 177 ORFs (82%)	58,500	YKH229	192,534	233 seq. (15%), 127 ORFs (59%)
3b			143,308	1,435 seq. (91%), 211 ORFs (98%)	pKH51	2	133,050	1,082 seq. (67%), 196 ORFs (91%)	32,000	YKH230	276,358	265 seq. (17%), 135 ORFs (63%)
4a	P1C, 1.0 ng (20 fmol)	pool-FP3 + pool-RP3	179,709	1,399 seq. (89%), 211 ORFs (98%)	pKH51	3	60,323	1,033 seq. (66%), 191 ORFs (89%)	90,500	YKH233	240,032	812 seq. (51%), 197 ORFs (92%)
4b			202,657	1,347 seq. (85%), 211 ORFs (98%)	pKH51	3	52,332	964 seq. (61%), 189 ORFs (98%)	95,000	YKH234	254,989	835 seq. (53%), 197 ORFs (92%)

Supplementary Table 2. Library statistics P2 (Fig. 4) & P3 (Fig. 5). * = DADA2 de-noising, considering only perfectly matched reads to the reference.

ID	oligo pool	PCR			feature cassette	SIC pool (after recombineering, RCA)			clone collections (libraries)			
		primer	reads mapped	identified unique sequences, ORFs		pooled RCA reactions	reads mapped	identified, unique sequences, ORFs	clones	library stock	reads mapped	identified unique sequences, ORFs
#1.1	P2, 1 x 80 pg (1.5 fmol)	pool-FP1 + pool-RP1	1,610,291	3,802 seq.* (30%), 2,985 ORFs (53%)	pMaM505 (kanMX)	4	3,066,702	3,196 SICs* (26%), 2,522 ORFs (45%)	109,000	YDK553 + YDK557	28,574,949	2,052 ORFs (36%)
#1.2					pBeB019 (hphNT1)	4	n. d.	n. d.	100,000	YDK556 + YDK483	28,619,645	2,317 ORFs (35%)
#1.3	P2, 10 x 80 pg (1.5 fmol)	pool-FP1 + pool-RP1	18,009,833	8,110 seq.* (65%), 5,025 ORFs (89%)	pBeB019 (hphNT1), 1/10 of PCR	4	n. d.	n d.	76,500	YDK559	22,476,787	2,033 ORFs (36%)
#2.111	P3, 1 x 2 ng (40 fmol)	pool-FP2 + pool-RP2	5,235,125	24,331 seq. (90%), 5,822 ORFs (98%)	pBeB064 (kanMX)	10	2,752,420	8,793 seq. (32%), 4,114 ORFs (69%)	17,000	YKG5	1,861,715	4,141 seq. (15%), 2,410 ORFs (40%)
#2.112									272,000	YKG7	26,138,518	6,531 seq. (24%), 3,241 ORFs (54%)
#2.211			5,773,501	23,918 seq. (88%), 5,791 ORFs (96%)	pBeB064 (kanMX)	10	1,786,215	5,832 seq. (22%), 3,076 ORFs (52%)	11,000	YKG8	1,001,235	4,151 seq. (15%), 2,466 ORFs (42%)
#2.212									172,000	YKG10	7,943,998	2,814 seq. (10%), 1,677 ORFs (28%)
#2.221					pBeB064 (kanMX)	10	2,335,370	8,441 seq. (31%), 3,844 (65%)	16,000	YKG11	1,143,105	1,839 seq. (6.8%), 1,391 ORFs (24%)
#2.222									260,000	YKG13	18,909,849	4,019 seq. (15%), 2,193 ORFs (37%)
#2.3			4,425,0238	2,3167 seq. (86%), 5,736 ORFs (95%)	pKH51 (hphNT1)	2	2,188,868	15,231 seq. (56%), 5,238 ORFs (88%)	116,000	YKH225	10,006,829	5,285 seq. (19%), 3,008 ORFs (51%)

Supplementary Table 3. Newly characterized ORFs in terms of protein abundance. Detection probability is a function of relative abundance of a clone in a (sub-)library (or 'bin'), selectivity of the phenotype enrichment protocol and accuracy of genotype identification. For each ORF identified after Oxford Nanopore NGS, read counts (> 1 count; 6 ORFs with 1 count only not shown) and fold enrichment (or depletion) with respect to the first FACS enrichment to purify the fluorescent portion (Illumina NGS) are shown. Only enriched loci were considered as hits. ORFs for which abundance information was available outside genome-scale experiments[10] are asterisked.

bin	enriched loci			depleted loci		
	systematic name	counts	fold	systematic name	counts	fold
bin 1, darkest 25% (2 ORFs)	*YMR105W-A*	2	12.1 x	*YMR175W-A**	6	0.35 x
	YGR204C-A	58	2.0 x			
bin 2, bright 40% (3 ORFs)	*YPL038W-A**	22	2.7 x	*YOL164W **	6	0.23 x
	*YOL156W**	16	4.4 x			
	YOR072W-B	6	1.3 x			
bin 3, brighter 25% (6 ORFs)	*YGR146C-A*	522	3.9 x	*YJR151W-A*	143	0.24 x
	YML054C-A	454	4.8 x	*YGR240C-A*	8	0.22 x
	YGL006W-A	15	10.3 x	*YBR298C-A*	6	0.39 x
	*YMR230W-A**	12	3.1 x	*YOR376W-A*	4	0.68 x
	*YDR194W-A**	5	4.5 x	*YJL136W-A*	2	0.71 x
bin 4, brightest 10% (1 ORF)	*YBR196C-A**	797	4.2 x	*YAL063C-A*	2	0.20 x

Supplementary Table 4. Strains used in this study.

strain	background	description	purpose	source
ESM356-1	S228C	MAT**a** ura3-52 leu2Δ1 his3Δ200 trp1Δ63	auxotrophic laboratory yeast strain	Ref.[11]
YBeB500	ESM356-1	*ura3-52*::GAL1pr-FnCpf1::NLS::3xHA-CYC1t (natNT2)	inducible expression in yeast (use discouraged for risk of gene-drive)	this work
YBeB600	ESM356-1	*ura3-52*::GAL1pr-LbCpf1::NLS::3xHA-CYC1t (natNT2)	inducible expression in yeast (use discouraged for risk of gene-drive)	this work
YBeB700	ESM356-1	*ura3-52*::GAL1pr-AsCpf1::NLS::3xHA-CYC1t (natNT2)	inducible expression in yeast (use discouraged for risk of gene-drive)	this work
YBeB800	ESM356-1	*ura3-52*::GAL1pr-MbCpf1::NLS::3xHA-CYC1t (natNT2)	inducible expression in yeast (use discouraged for risk of gene-drive)	this work

Supplementary Table 5. Plasmids used in this study.

plasmid	backbone	description	purpose	source
pY004	pcDNA 3.1(+)	CMVpr-hFnCpf1::NLS ::3xHA::bGH poly(A)	mammalian expression	Ref.[2]
pY010	pcDNA 3.1(+)	CMVpr-hAsCpf1::NLS ::3xHA::bGH poly(A)	mammalian expression	Ref.[2]
pY014	pcDNA 3.1(+)	CMVpr-hMbCpf1::NLS ::3xHA::bGH poly(A)	mammalian expression	Ref.[2]
pY016	pcDNA 3.1(+)	CMVpr-hLbCpf1::NLS ::3xHA::bGH poly(A)	mammalian expression	Ref.[2]
pRS306N		shuttle vector and yeast integrating plasmid at *ura3-52* conferring nourseothricin resistance		Ref.[12]
pMaM486	pRS306N	GAL1pr-hFnCpf1::NLS ::3xHA-CYC1t	stable genomic integration in yeast, inducible expression	this work
pMaM487	pRS306N	GAL1pr-hAsCpf1::NLS ::3xHA-CYC1t	stable genomic integration in yeast, inducible expression	this work
pMaM488	pRS306N	GAL1pr-hMbCpf1::NLS ::3xHA-CYC1t	stable genomic integration in yeast, inducible expression	this work
pMaM489	pRS306N	GAL1pr-hLbCpf1::NLS ::3xHA-CYC1t	stable genomic integration in yeast, inducible expression	this work
pRS416		shuttle vector and yeast centromeric plasmid conferring uracil prototrophy		Ref.[13]

(Supplementary Table 5 continued)

plasmid	backbone	description	purpose	source
pRS415		shuttle vector and yeast centromeric plasmid conferring leucine prototrophy		Ref.[13]
pBeB503	pRS416	TEF1pr-hFnCpf1::NLS::3xHA-CYC1t	constitutive expression in yeast	this work
pBeB603	pRS416	TEF1pr-hLbCpf1::NLS::3xHA-CYC1t	constitutive expression in yeast	this work
pBeB703	pRS416	TEF1pr-hAsCpf1::NLS::3xHA-CYC1t	constitutive expression in yeast	this work
pBeB803	pRS416	TEF1pr-hMbCpf1::NLS::3xHA-CYC1t	constitutive expression in yeast	this work
pBeB501	pRS415	GAL1pr-hFnCpf1::NLS::3xHA-CYC1t	inducible expression in yeast	this work
pBeB601	pRS415	GAL1pr-hLbCpf1::NLS::3xHA-CYC1t	inducible expression in yeast	this work
pBeB701	pRS415	GAL1pr-hAsCpf1::NLS::3xHA-CYC1t	inducible expression in yeast	this work
pBeB801	pRS415	GAL1pr-hMbCpf1::NLS::3xHA-CYC1t	inducible expression in yeast	this work
pFA6a		*E. coli* plasmid with ampicillin resistance gene *amp*R		Ref.[14]
pBeB019	pFA6a	S3-mScarlet-i-ADH1t (hphNT1) SNR52pr-FnCpf1 handle	feature cassette template with a GFP conferring hygromycin resistance	this work
pBeB013	pFA6a	S3-mNeonGreen-ADH1t (hphNT1) SNR52pr-FnCpf1 handle	feature cassette template with a GFP conferring hygromycin resistance	this work
pMaM505	pFA6a	S3-mNeonGreen-ADH1t (kanMX4) SNR52pr-FnCpf1 handle	feature cassette template with a GFP conferring G-418 resistance	this work
pBeB064	pFA6a	mNeonGreen-ADH1t(kanMX4) SNR52pr-t(GCC)F1-FnCpf1 handle	feature cassette template with a GFP conferring G-418 resistance	this work
pKH51	pFA6a	mNeonGreen-ADH1t(hphNT1) SNR52pr-t(GCC)F1-FnCpf1 handle	feature cassette template with a GFP conferring hygromycin resistance	this work

Supplementary Table 6. 1,577 oligonucleotide pool sequences for the small library targeting 215 nuclear proteins with nuclear localization. Table provided as Online Supplementary Material.

Supplementary Table 7. Oligonucleotide pool sequences for the first genome-wide library by ORF. Some of the unique set of 12,472 sequences can target more than a single ORF, which is why a total number of 12,514 entries is provided. We excluded seven entries for *YEL020W-A*, *YEL020C-B*, *YEL021W*, and *YEL022W*, which are near to *ura3*-52, the locus at which the Cas12a-family proteins were integrated in this study (Supplementary Note). Table provided as Online Supplementary Material.

Supplementary Table 8. Oligonucleotide pool sequences for the second genome-wide library by ORF. Some of the unique set of 27,000 sequences can target more than a single ORF, which is why a total number of 27,640 entries is provided. We excluded 15 entries for *YEL020W-A*, *YEL020C-B*, *YEL021W*, and *YEL022W*, which are near to *ura3*-52, the locus at which the Cas12a-family proteins were integrated in this study (Supplementary Note). Table provided as Online Supplementary Material.

Supplementary Table 9. Primers used in this study.

primer name	primer sequence (5'-to-3')
S3-GPD1-BamHI	CTATGGATCCAAGAACCTGCCGGACATGATTGAAGAATTAGATCTACATGAAGATCGTACG CTGCAGGTCGAC
GPD1 3'-HA with FnCpf1 [crRNA]GPD1+1182	ATAGGATCCGTGGGGGAAAGTATGATATGTTATCTTTCTCCAATAAATCTAAAAAAAAAGAT ATGTTATCTTTCTCCAAATCTACAACAGTAGAAATTAGATCATTTATCTTTCACTGCGG
S3-PIL1-BamHI	CTATGGATCCGTCGGACACCAGCAAAGTGAGTCTCTTCCCCAACAAACAACAGCTCGTACG CTGCAGGTCGAC
PIL1 3'-HA with FnCpf1 [crRNA]PIL1+1022	ATAGGATCCTTTTTTTTTTTGTTTCTAATAGATTGTTGATTTATTTTGATTAAAAAAAACAA CAAACAACAGCTTAATCATCTACAACAGTAGAAATTAGATCATTTATCTTTCACTGCGG
S3-MDH1-BamHI	CTATGGATCCTTGAAGAAGAATATCGAAAAGGGTGTCAACTTTGTTGCTAGTAAACGTACG CTGCAGGTCGAC
MDH1 3'-HA with FnCpf1 [crRNA]MDH1+998	ATAGGATCCTTTTCCCTATTTTTCACTCTATTTCTGATCTTGAACAATCTAAAAAAAAGGT GTCAACTTTGTTGCTAGATCTACAACAGTAGAAATTAGATCATTTATCTTTCACTGCGG
S3-ENO2-BamHI	CTATGGATCCAAGGCTGTCTACGCCGGTGAAAACTTCCACCACGGTGACAAGTTGCGTACG CTGCAGGTCGAC
ENO2 3'-HA with FnCpf1 [crRNA]ENO2+1311	ATAGGATCCATAAGCAGAAAAGACTAATAATTCTTAGTTAAAAGCACTTTAAAAAAAATCC ACCACGGTGACAAGTTGATCTACAACAGTAGAAATTAGATCATTTATCTTTCACTGCGG
ENO2 3'-HA with FnCpf1 [crRNA]ENO2+1329	ATAGGATCCATAAGCAGAAAAGACTAATAATTCTTAGTTAAAAGCACTTTAAAAAAAATGT AAAGTGCTTTTAACTAAATCTACAACAGTAGAAATTAGATCATTTATCTTTCACTGCGG
ENO2 3'-HA with AsCpf1 [crRNA]ENO2+1329	ATAGGATCCATAAGCAGAAAAGACTAATAATTCTTAGTTAAAAGCACTTTAAAAAAAATCC ACCACGGTGACAAGTTGATCTACAAGAGTAGAAATTAGATCATTTATCTTTCACTGCGG
ENO2 3'-HA with MbCpf1 [crRNA]ENO2+1329	ATAGGATCCTAAGCAGAAAAGACTAATAATTCTTAGTTAAAAGCACTTTAAAAAAAATCCA CCACGGTGACAAGTTGATCTACAAACAGTAGAAATTTGATCATTTATCTTTCACTGCGG
ENO2 3'-HA with LbCpf1 [crRNA]ENO2+1329	ATAGGATCCTAAGCAGAAAAGACTAATAATTCTTAGTTAAAAGCACTTTAAAAAAAATCCA CCACGGTGACAAGTTGATCTACACTTAGTAGAAATTAGATCATTTATCTTTCACTGCGG
S3-PDC1-BamHI	CTATGGATCCTTGGTTGAACAAGCTAAGTTGACTGCTGCTACCAACGCTAAGCAACGTACG CTGCAGGTCGAC
PDC1 3'-HA with FnCpf1 [crRNA]PDC1+1701	ATAGGATCCGCTTATAAAACTTTAACTAATAATTAGAGATTAAATCGCTTAAAAAAAATTT AACTAATAATTAGAGATATCTACAACAGTAGAAATTAGATCATTTATCTTTCACTGCGG
PDC1 3'-HA with FnCpf1 [crRNA]ADE2+241	ATAGGATCCGCTTATAAAACTTTAACTAATAATTAGAGATTAAATCGCTTAAAAAAAAGCA TGTTGATGTTCCTACACATCTACAACAGTAGAAATTAGATCATTTATCTTTCACTGCGG
PDC1 3'-HA with FnCpf1 [crRNA]PDC1+1705	ATAGGATCCGCTTATAAAACTTTAACTAATAATTAGAGATTAAATCGCTTAAAAAAAAGCA ATAAGCGATTTAATCTCATCTACAACAGTAGAAATTAGATCATTTATCTTTCACTGCGG
PDC1 3'-HA with AsCpf1 [crRNA]PDC1+1701	ATAGGATCCGCTTATAAAACTTTAACTAATAATTAGAGATTAAATCGCTTAAAAAAAATTT AACTAATAATTAGAGATATCTACAAGAGTAGAAATTAGATCATTTATCTTTCACTGCGG
PDC1 3'-HA with MbCpf1 [crRNA]PDC1+1701	ATAGGATCCCTTATAAAACTTTAACTAATAATTAGAGATTAAATCGCTTAAAAAAAATTTA ACTAATAATTAGAGATATCTACAAACAGTAGAAATTTGATCATTTATCTTTCACTGCGG
PDC1 3'-HA with LbCpf1 [crRNA]PDC1+1701	ATAGGATCCCTTATAAAACTTTAACTAATAATTAGAGATTAAATCGCTTAAAAAAAATTTA ACTAATAATTAGAGATATCTACACTTAGTAGAAATTAGATCATTTATCTTTCACTGCGG
pool-FP1	GATAAATGATCTAATTTCTACTGTTGTAG
pool-RP1	AGTAGAAGTATTGCCGGC
pool-FP2	GGGCTTGCGCATAATTTCTACTGTTGTAGAT
pool-RP2	ACGACCGCCTGAAGAGCC
pool-FP3	GGGCTTGCGCATAATTTCTACTGTTGTAG
pool-RP3	GTGCACCGCCTGAAGAGCC
cassette-FP1	GCCGGCAATACTTCTACTCGTACGCTGCAGGTCGAC
cassette-RP1	ATCTACAACAGTAGAAATTAGATCATTTATCTTTC

cassette-FP2 (-FP3)	GGCTCTTCAGGCGGTGCACGTACGCTGCAGGTCGAC
cassette-RP2 (-RP3)	ATCTACAACAGTAGAAATTATGCGCAAGCCC
vect_bubble-no_BC-Watson	/PHOS/CGTCCTCTCCTGCTCTGTAGCCTTCTCGTGTGCAGACTTGAGGTGAGTGGCTCTC TTCCCTCT/3DDC/
vect_bubble-no_BC-Crick	CCGAGAGGGAAGAGAGCGTGACTGGAGTTCAGACGTGTGCTCTTCCGATCTGAGCAGGAGA GGACGT
vect_bubble-BC1-Watson	/PHOS/GAGAAGCAACGTCCTCTCCTGCTCTGTAGCCTTCTCGTGTGCAGACTTGAGGTGA GTGGCTCTCTTCCCTCT/3DDC/
vect_bubble-BC1-Crick	CCGAGAGGGAAGAGAGCGTGACTGGAGTTCAGACGTGTGCTCTTCCGATCTGAGCAGGAGA GGACGTTGCTTCTCT
vect_bubble-BC2-Watson	/PHOS/CTTACCGCTCGTCCTCTCCTGCTCTGTAGCCTTCTCGTGTGCAGACTTGAGGTGA GTGGCTCTCTTCCCTCT/3DDC/
vect_bubble-BC2-Crick	CCGAGAGGGAAGAGAGCGTGACTGGAGTTCAGACGTGTGCTCTTCCGATCTGAGCAGGAGA GGACGAGCGGTAAGT
vect_bubble-BC3-Watson	/PHOS/ACTCTCAAGCGTCCTCTCCTGCTCTGTAGCCTTCTCGTGTGCAGACTTGAGGTGA GTGGCTCTCTTCCCTCT/3DDC/
vect_bubble-BC3-Crick	CCGAGAGGGAAGAGAGCGTGACTGGAGTTCAGACGTGTGCTCTTCCGATCTGAGCAGGAGA GGACGCTTGAGAGTT
vect_bubble-BC4-Watson	/PHOS/CCAACAGAACGTCCTCTCCTGCTCTGTAGCCTTCTCGTGTGCAGACTTGAGGTGA GTGGCTCTCTTCCCTCT/3DDC/
vect_bubble-BC4-Crick	CCGAGAGGGAAGAGAGCGTGACTGGAGTTCAGACGTGTGCTCTTCCGATCTGAGCAGGAGA GGACGTTCTGTTGGT
vect_initiating_primer	GTTCAGACGTGTGCTCTTCCG
vect_specific-mNeon-BC1	ACACTCTTTCCCTACACGACGCTCTTCCGATCTNNNNNNNNCGCTAACTCGCCATGTTGTC TTCTTCACC
vect_specific-mNeon-BC2	ACACTCTTTCCCTACACGACGCTCTTCCGATCTNNNNNNNNGAGAGACCACTGCCATGTTG TCTTCTTCACC
vect_specific-mNeon-BC3	ACACTCTTTCCCTACACGACGCTCTTCCGATCTNNNNNNNNCCAGAAGAAGCCATGTTGTC TTCTTCACC
vect_specific-mScarlet-BC1	ACACTCTTTCCCTACACGACGCTCTTCCGATCTNNNNNNNNAACCTTGTCGCTCCTTGATC ACTGCCTCGC
vect_specific-mScarlet-BC2	ACACTCTTTCCCTACACGACGCTCTTCCGATCTNNNNNNNNTGTGTCCGTCTCCTTGATCA CTGCCTCGC
vect_specific-SNR52-BC1	ACACTCTTTCCCTACACGACGCTCTTCCGATCTNNNNNNNNCAATCCGCAAGCAGTGAAAG ATAAATGATCTAATTTCTACTG
vect_specific-SNR52-BC2	ACACTCTTTCCCTACACGACGCTCTTCCGATCTNNNNNNNNGCGTATTGAGCAGTGAAAGA TAAATGATCTAATTTCTACTG
vect_specific-SNR52-BC3	ACACTCTTTCCCTACACGACGCTCTTCCGATCTNNNNNNNNGCAACGTTCAGCAGTGAAAG ATAAATGATCTAATTTCTACTG
vect_specific-SNR52-BC4	ACACTCTTTCCCTACACGACGCTCTTCCGATCTNNNNNNNNATCTGGAGTTAGCAGTGAAA GATAAATGATCTAATTTCTACTG
vect_illumina-P5	AATGATACGGCGACCACCGAGATCTACACTCTTTCCCTACACGACGCTC
vect_illumina-P7	CAAGCAGAAGACGGCATACGAGATGGCCACTGTGACTGGAGTTCAGACGTGTGCTCTTCCG ATC
halfY-Rd2-Watson	/PHOS/CGTCCTCTCCTGCTC/SPCC3/
halfY-Rd2-N8-Crick	GATCGATCGATCGTTCAGACGTGTGCTCTTCCGATCTNNNNNNNN(TT)GAGCAGGAGAGG ACGT
halfY-Rd2-N8T-Crick	GATCGATCGATCGTTCAGACGTGTGCTCTTCCGATCTNNNNNNNNTGAGCAGGAGAGGACG T

halfY-Rd2-N8T2-Crick	GATCGATCGATCGTTCAGACGTGTGCTCTTCCGATCTNNNNNNNNTTGAGCAGGAGAGGAC GT
Vect_specific-FnCpf1-handle-N6	ACACTCTTTCCCTACACGACGCTCTTCCGATCTNNNNNNCTTGCGCATAATTTCTACTGTT G
Vect_specific-FnCpf1-handle-N6G	ACACTCTTTCCCTACACGACGCTCTTCCGATCTNNNNNNGCTTGCGCATAATTTCTACTGT TG
Vect_specific-FnCpf1-handle-N6G2	ACACTCTTTCCCTACACGACGCTCTTCCGATCTNNNNNNGGCTTGCGCATAATTTCTACTG TTG
tRNA-seq-N6.fw	ACACTCTTTCCCTACACGACGCTCNNNNNNGTTCGATTCCGGGCTTG
tRNA-seq-N6T.fw	ACACTCTTTCCCTACACGACGCTCNNNNNNTGTTCGATTCCGGGCTTG
tRNA-seq-N6T2.fw	ACACTCTTTCCCTACACGACGCTCNNNNNNTTGTTCGATTCCGGGCTTG
mNeon-seq-N6.rev	GTTCAGACGTGTGCTCTTCCGATCTNNNNNNGTCTTCTTCACCCTTAGAAACC
mNeon-seq-N6T.rev	GTTCAGACGTGTGCTCTTCCGATCTNNNNNNTGTCTTCTTCACCCTTAGAAACC
mNeon-seq-N6T2.rev	GTTCAGACGTGTGCTCTTCCGATCTNNNNNNTTGTCTTCTTCACCCTTAGAAACC
P023poolseqN6.fw	ACACTCTTTCCCTACACGACGCTCNNNNNNGGGCTTGCGCATAATTTC
P023poolseqN6T.fw	ACACTCTTTCCCTACACGACGCTCNNNNNNTGGGCTTGCGCATAATTTC
P023poolseqN6T2.fw	ACACTCTTTCCCTACACGACGCTCNNNNNNTTGGGCTTGCGCATAATTTC
P023poolseqN6.rv	GTTCAGACGTGTGCTCTTCCGATCTNNNNNNGTGCACCGCCTGAAGAG
P023poolseqN6T.rv	GTTCAGACGTGTGCTCTTCCGATCTNNNNNNTGTGCACCGCCTGAAGAG
P023poolseqN6T2.rv	GTTCAGACGTGTGCTCTTCCGATCTNNNNNNTTGTGCACCGCCTGAAGAG
III-ONP-P5-bi501	AATGATACGGCGACCACCGAGATCTACACTGTGGCGCAAGCTTACACTCTTTCCCTACACG ACGCTC
III-ONP-P5-bi502	AATGATACGGCGACCACCGAGATCTACACCGCGATCTAGGAAGACACTCTTTCCCTACACG ACGCTC
III-ONP-P5-bi503	AATGATACGGCGACCACCGAGATCTACACAATGACGAGCGAATACACTCTTTCCCTACACG ACGCTC
III-ONP-P5-bi504	AATGATACGGCGACCACCGAGATCTACACTCAGAACTCTCGAAACACTCTTTCCCTACACG ACGCTC
III-ONP-P5-bi505	AATGATACGGCGACCACCGAGATCTACACTTCCTACGAACAGAACACTCTTTCCCTACACG ACGCTC
III-ONP-P5-bi506	AATGATACGGCGACCACCGAGATCTACACATTCGGTTGCCTAGACACTCTTTCCCTACACG ACGCTC
III-ONP-P5-bi507	AATGATACGGCGACCACCGAGATCTACACCACATAACAGTTGGACACTCTTTCCCTACACG ACGCTC
III-ONP-P5-bi508	AATGATACGGCGACCACCGAGATCTACACGTGGATTCTCCAGTACACTCTTTCCCTACACG ACGCTC
III-ONP-P5-bi509	AATGATACGGCGACCACCGAGATCTACACACCTTCTCGATGGAACACTCTTTCCCTACACG ACGCTC
III-ONP-P5-bi510	AATGATACGGCGACCACCGAGATCTACACCTCTCCTTCCGGTTACACTCTTTCCCTACACG ACGCTC
III-ONP-P7-bi701	CAAGCAGAAGACGGCATACGAGATTGTGGCGCAAGCTTGTGACTGGAGTTCAGACGTGTGC TCTTCCGATC
III-ONP-P7-bi702	CAAGCAGAAGACGGCATACGAGATCGCGATCTAGGAAGGTGACTGGAGTTCAGACGTGTGC TCTTCCGATC
III-ONP-P7-bi703	CAAGCAGAAGACGGCATACGAGATAATGACGAGCGAATGTGACTGGAGTTCAGACGTGTGC TCTTCCGATC
III-ONP-P7-bi704	CAAGCAGAAGACGGCATACGAGATTCAGAACTCTCGAAGTGACTGGAGTTCAGACGTGTGC TCTTCCGATC

III-ONP-P7-bi705	CAAGCAGAAGACGGCATACGAGATTTCCTACGAACAGAGTGACTGGAGTTCAGACGTGTGC TCTTCCGATC
III-ONP-P7-bi706	CAAGCAGAAGACGGCATACGAGATATTCGGTTGCCTAGGTGACTGGAGTTCAGACGTGTGC TCTTCCGATC
III-ONP-P7-bi707	CAAGCAGAAGACGGCATACGAGATCACATAACAGTTGGGTGACTGGAGTTCAGACGTGTGC TCTTCCGATC
III-ONP-P7-bi708	CAAGCAGAAGACGGCATACGAGATGTGGATTCTCCAGTGTGACTGGAGTTCAGACGTGTGC TCTTCCGATC
III-ONP-P7-bi709	CAAGCAGAAGACGGCATACGAGATACCTTCTCGATGGAGTGACTGGAGTTCAGACGTGTGC TCTTCCGATC
III-ONP-P7-bi710	CAAGCAGAAGACGGCATACGAGATCTCTCCTTCCGGTTGTGACTGGAGTTCAGACGTGTGC TCTTCCGATC

Supplementary Table 10. Pool designs.

Oligo-pool ID	PAM space	degeneracy		oligo length	supplier
		sequences	ORFs		
P1A	TTV (1,577)	1,577	215 nuclear ORFs	160 nt	CustomArray Inc.
P1B					Twist Bioscience
P1C					Twist Bioscience
P2	TTV (11,155) +TYN (1,317)	12,472	5,664	170 nt	CustomArray Inc.
P3	TTV (27,000)	27,000	5,940	160 nt	Agilent Technologies

References.

1. Engel, S. R. *et al.* The reference genome sequence of Saccharomyces cerevisiae: then and now. *G3* **4,** 389–398 (2014).
2. Zetsche, B. *et al.* Cpf1 is a single RNA-guided endonuclease of a class 2 CRISPR-Cas system. *Cell* **163,** 759–771 (2015).
3. Sinkins, S. P. & Gould, F. Gene drive systems for insect disease vectors. *Nat Rev Genet* **7,** 427–435 (2006).
4. Hammond, A. *et al.* A CRISPR-Cas9 gene drive system targeting female reproduction in the malaria mosquito vector Anopheles gambiae. *Nat Biotechnol* **34,** 78–83 (2016).
5. Committee on Gene Drive Research in Non-Human Organisms: Recommendations for Responsible Conduct, Board on Life Sciences, Division on Earth and Life StudiesNational Academies of Sciences, Engineering, and Medicine. Gene Drives on the Horizon: Advancing Science, Navigating Uncertainty, and Aligning Research with Public Values. (2016). doi:10.17226/23405
6. Esvelt, K. M., Smidler, A. L., Catteruccia, F. & Church, G. M. Concerning RNA-guided gene drives for the alteration of wild populations. *Elife* **3,** 20131071 (2014).
7. Zhang, L., Kasif, S., Cantor, C. R. & Broude, N. E. GC/AT-content spikes as genomic punctuation marks. *Proc Natl Acad Sci USA* **101,** 16855–16860 (2004).
8. Kaplan, N. *et al.* The DNA-encoded nucleosome organization of a eukaryotic genome. *Nature* **458,** 362–366 (2009).
9. Jordán-Pla, A. *et al.* Chromatin-dependent regulation of RNA polymerases II and III activity throughout the transcription cycle. *Nucl Acids Res* **43,** 787–802 (2015).
10. Wang, M. *et al.* PaxDb, a database of protein abundance averages across all three domains of life. *Mol. Cell Proteomics* **11,** 492–500 (2012).
11. Knop, M. & Schiebel, E. Receptors determine the cellular localization of a γ-tubulin complex and thereby the site of microtubule formation. *EMBO J* **17,** 3952–3967 (1998).
12. Taxis, C. & Knop, M. System of centromeric, episomal, and integrative vectors based on drug resistance markers for Saccharomyces cerevisiae. *BioTechniques* **40,** 73–78 (2006).
13. Sikorski, R. S. & Hieter, P. A system of shuttle vectors and yeast host strains designed for efficient manipulation of DNA in Saccharomyces cerevisiae. *Genetics* **122,** 19–27 (1989).
14. Wach, A., Brachat, A., Pöhlmann, R. & Philippsen, P. New heterologous modules for classical or PCR-based gene disruptions in Saccharomyces cerevisiae. *Yeast* **10,** 1793–1808 (1994).